Universiteit Utrecht

Paleolatitude and paleospreading directions recovered from the Oman ophiolite.

Louise M.T. Koornneef

Earth Sciences – Earth, Structure, and Dynamics – Master Thesis – 31-03-2016 – Utrecht University

Supervised by Dr. Douwe J.J. van Hinsbergen and Dr. Marco Maffione

---

Abstract - A ~8000 km wide ocean called the Neo-Tethys Ocean disappeared underneath the Eurasian plate during long time plate convergence between India and Eurasia since 130 Ma ago (and likely even earlier). The only rock records that are left of the large Tethyan ocean are ophiolitic belts that are nowadays found on top of the continents. The Semail ophiolite in Oman is one of them, and has formed while the Indian plate moved in a NE direction to collide with the Eurasian plate. Nowadays the Semail ophiolite forms a 500 km long belt composed a complete ophiolitic sequence of mantle rocks, gabbros, sheeted dykes, lava flows, and deep marine sediments, making it the most intact and most thoroughly studied ophiolite in the past 30 years.

The aim of this study is (i) to find the amount of rotation around a vertical axis experienced by the ophiolite, and (ii) to find the paleospreading direction of the oceanic ridge during the formation of the ophiolite, as well as along what kind of plate boundary the ophiolite formed. Paleomagnetic analyses of the upper crustal sequence (sheeted dykes and pillow lavas) of the Oman ophiolite was the adopted technique to reconstruct the initial orientations of the spreading ridges, determining their paleodirection and rotation, as well as the paleolatitude at which the ophiolite formed. In this work more than 400 cores from 12 localities were paleomagnetically analysed through both alternating field and thermal demagnetization treatments. Remanence components were isolated using standard paleomagnetic techniques and the mean values were calculated via Fisherian statistics of the characteristic remanence magnetisations. We used a Net Tectonic Rotation approach to calculate the rotation pattern and establish the initial dyke orientation necessary to infer on the paleospreading directions, for dykes are formed parallel to the spreading ridge. The results of this analysis evidenced the presence of two sectors rotated in opposite directions: clockwise in the northern and middle part of the ophiolite, and counterclockwise in the eastern part. Using NTR analysis we also documented the spreading directions, which are perpendicular to the N-S strike found for the magmatic spreading centres obtained from the initial orientation of the sheeted dykes. From the pillow lavas a paleolatitude of 8.6° N was found for the ophiolites at the moment of formation. From the found pattern, with both CW and CCW rotation, a N-S strike of the spreading ridge, and the paleolatitude, we argue that the ophiolite was not formed along a Neo-Tehyan ocean spreading ridge, but rather along a N-S transform segment of the western limit of the Indian plate, above a newly initiated subduction zone.

1 Introduction

The Semail ophiolite in Oman is the best preserved and largest thrust sheet of oceanic crust and upper mantle in the world (550 km long, 150 km wide, with a total area of 10.000 km^2), and therefore also the most extensively studied (Lippard et al., 1986; Thomas et al., 1987; Nicolas et al., 1988). The ophiolitic nappe is divided into 12 parts that have been given names after local mountains and wadis (rivers) that are given in Figure 1. Ten of those parts (most of the ophiolite) lie in Oman and have been studied in great detail. Many scientists have tried to reconstruct the evolution of the Oman ophiolites in terms of tectonic rotations, paleolatitude, and spreading directions, often achieving contrasting conclusions (Thomas et al., 1987; Perrin et al., 1994, 2000; Feinberg et al., 1999; Nicolas et al., 1995). Of all these studies, much confusion still exists about the amount of rotation experienced by the ophiolites, as results from pillow lavas provide large rotation angles of 75-150° around a vertical rotation axis (Thomas et al., 1987; Perrin et al., 1994). It is also still not clear along what kind of plate boundary the ophiolite formed, yet most studies conclude that the ophiolite formed in the Neo-Tethys Ocean. Some scientists say that the formation of the ophiolite was initiated by thrusting and subduction along a spreading ridge (Nicolas et al., 1989), while some say the ophiolite was initiated in a supra-subduction back-arc context (Lippard et al., 1986). New information provided by other paleomagnetic methods is needed to find out which of these cases is true and to provide a new evolution model for the Oman ophiolite, for the hypotheses given in previous studies leave some questions unanswered; if the ophiolites formed close to a subduction zone or Neotethyan spreading ridge, then was there E-W or N-S oriented extension for the spreading ridges? A more general question that needs to be answered is, how did the Oman ophiolite evolve in terms of timing of rotations and tilt? In this study we address those questions by carrying out an extensive paleomagnetic analysis of the ophiolites of the Oman nappe at 12 locations spread over the whole Oman ophiolite. We investigate the geodynamics of spreading of the Oman ophiolite, to find out along what former plate boundary the Oman ophiolite formed, what its orientation was, and how much rotation took place between the moment of formation and the present day situation. In this study we also investigate the ophiolite's paleolatitude at the time of formation, based on data from pillow lavas.

Paleomagnetic analysis done on 12 sheeted dyke and pillow lava sites (Figure 1) provided the results presented in this study, using both alternating field and thermal demagnetisation. Rock magnetic analysis done on both the sheeted dykes and pillow lavas (thermomagnetic and susceptibility analysis, hysteresis loops and IRM curves, optical and SEM microscopy) supports this data.

2 Geological setting

The Semail Oman ophiolite consists of a large intact thrust slice that is composed of 4-7 km of oceanic crustal rocks and 8-12 km of upper mantle peridotites (Lippard et al., 1986; Nicolas, 1989). The ophiolitic sequence is complete and consists of (top to bottom) oceanic sediments (radiolarian cherts and umber), volcanics (pillow lavas and lava flows), a sheeted dyke complex, gabbros, peridotites, and the metamorphic sole. The lava flows consist of three different magmatic events; V1 ridge-axis basalts, V2 volcanics associated with the beginning of the thrusting, and V3 volcanics which formed immediately before the obduction of the ophiolite onto the continent (Ernewein et al., 1988).

The ophiolite was formed in the Cretaceous normal superchron that lasted from approximately 121-83 Ma, during the course of which short inversions might have taken place (Lowrie et al., 1980). The ophiolite is of a Late Cretaceous age, the age being obtained from U-Pb zircon ages from plagiogranites, ranging from 97.3 to 93.5 Ma (Tilton et al., 1981, Rioux et al., 2013). The time span of obduction of the ophiolite was found to be between 70 and 80 Ma, restricted by the ages of the youngest sediments below the nappe to the oldest sediments above (Ernewein et al., 1988).

The formation of the Oman ophiolites took place at the same time as subduction of the Indian plate beneath the Eurasian plate (in a forearc setting) took place (van Hinsbergen et al., 2012). It is possible that subduction zones were also present close to the Arabian continent. It is now known that ophiolites do not only form at mid-ocean ridges, but also above subduction zones, which in that case are classified as supra-subduction zone ophiolites (SSZ ophiolites) (Pearce et al., 1984; Pearce et al., 2003). Slab rollback happening during the early stage of subduction will lead to seafloor spreading close to the trench above the subduction zone, due to mantle wedge melting and crustal accretion.

2.1 Sampling

Figure 2 shows photographs of some of the sites and lithologies presented in this study. The sampled sites are located in different massifs distributed along the ophiolitic nappe of Oman, ranging from the Fizh block in the North of the nappe, to the Wadi Tayin block in the East of the nappe (Figure 1). The exact locations and lithologies of the sampled sites can be found in Table 1. The lithologies shown in the table result from observations in the field. Samples have been taken from 12 locations in total; one location with pillow lavas has been sampled (MA01-02) from the Shaik location (Figure 2 a), and samples were taken from 11 locations out of sheeted dykes (Figure 1) from the Wadi Tayin, Shaik, Sumail, Miskin, Haylayn, Sarami, Fizh, and Hilti locations (Figure 2 b-d). In total, over 400 cores were drilled in the field from the sheeted dykes and pillow lavas combined.

3 Analytical methods

Oriented cores (25 mm in diameter) were drilled in the Oman ophiolite using a gasoline-powered core drill and oriented with both magnetic and sun compasses. These cores were later cut into standard size specimens (25 mm in diameter, 22 mm in height) in the lab using a circular diamond dualblade saw. In this way, samples from the same core could be demagnetised (removing the low stability remanence components) using both the alternating field (AF) method and the thermal demagnetisation (TH) method in order to isolate characteristic remanent magnetisation (ChRM).

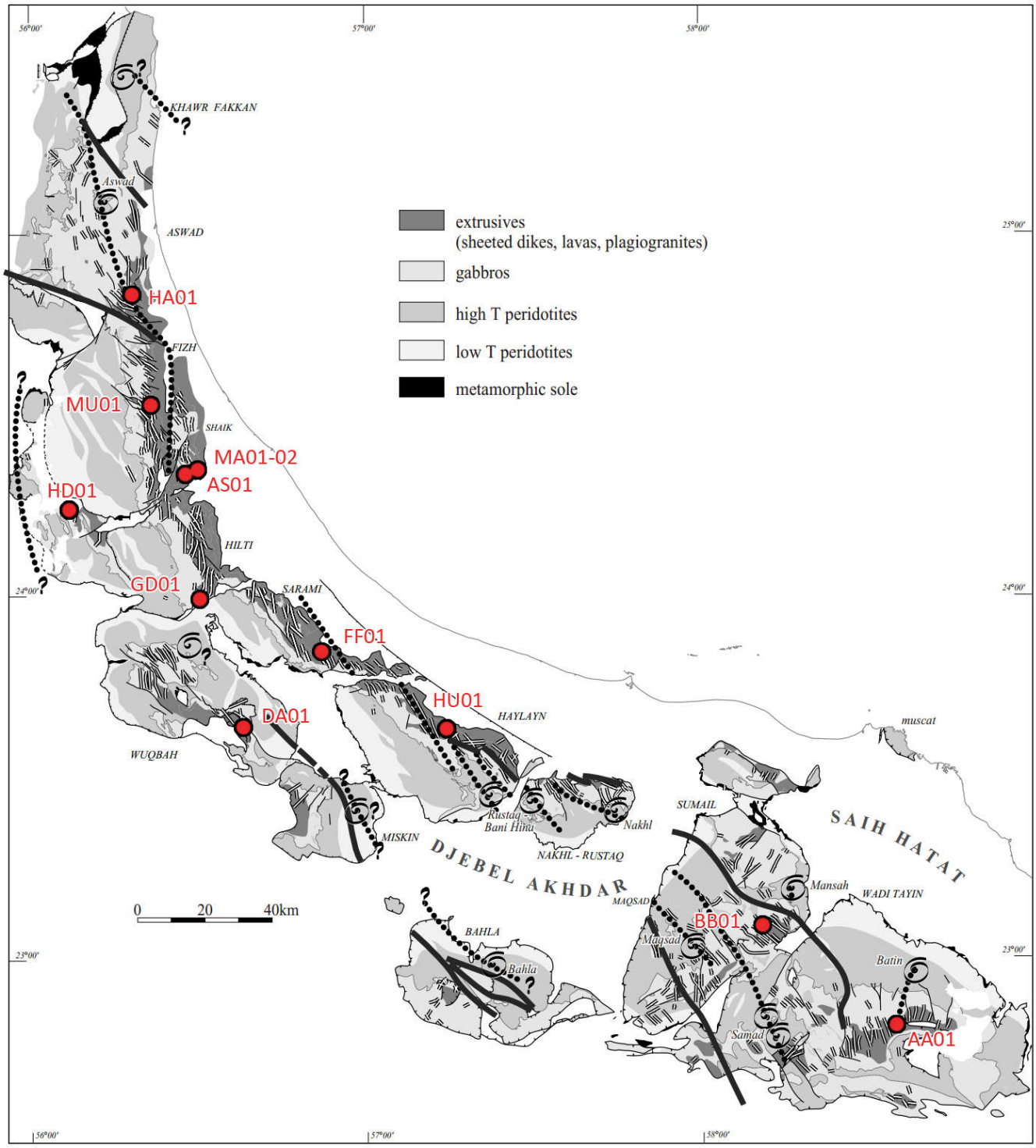

Figure 1. Simplified geological map of the ophiolite nappe in Oman (after Nicolas et al., 2000). Red dots show the locations of sites presented in this study. Different parts of the ophiolite are referred to by the name of their corresponding mountain or wadi (river), and are named as follows; Khawr Fakkan and Aswad (United Arab Emirates), Fizh, Hilti, Sarami, Wuqbah, Haylayn, Miskin, Nakhl-Rustaq, Bahla, Sumail, and Wadi Tayin (Oman).

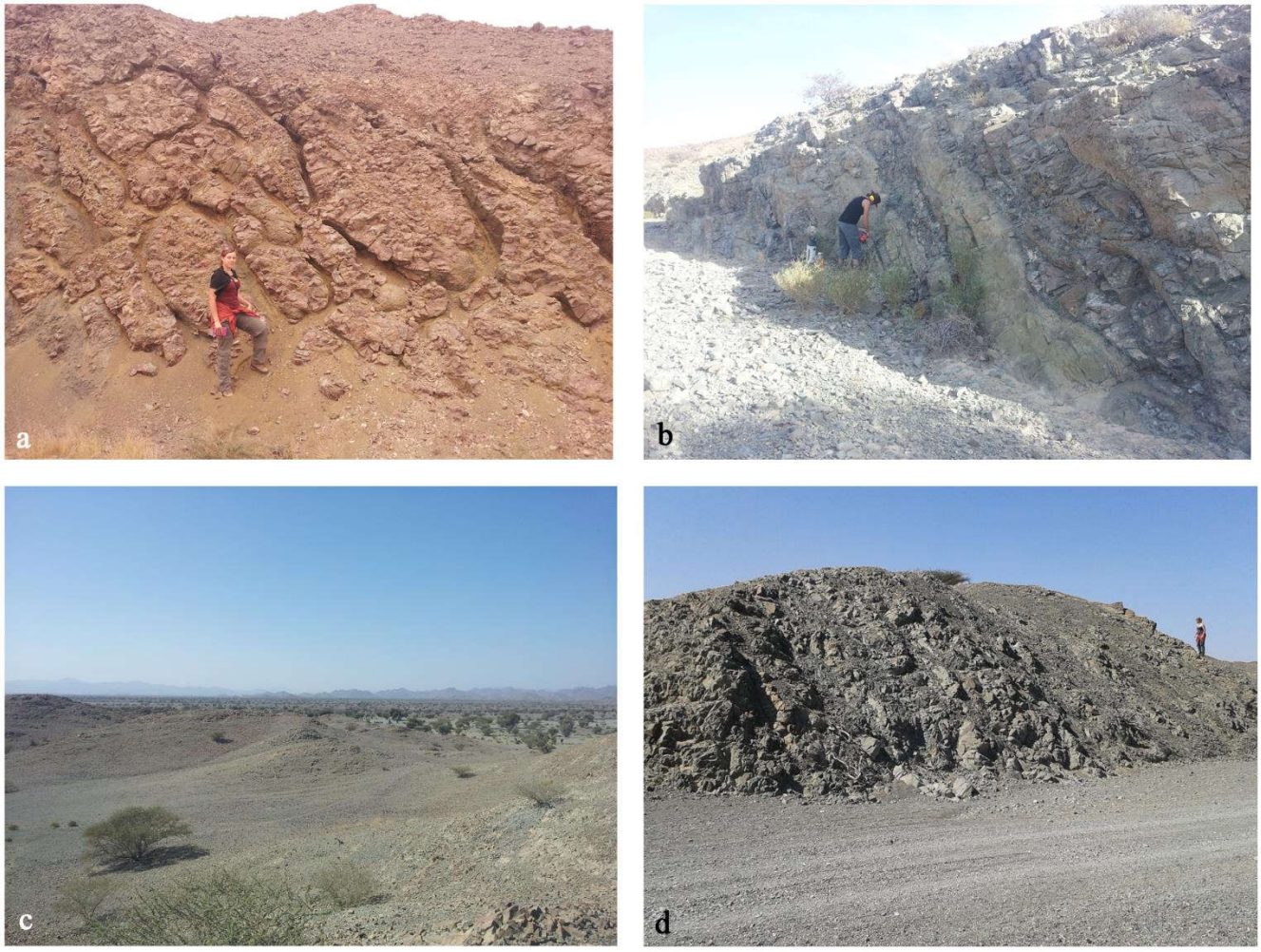

Figure 2. Photographs taken in the field. A) Pillow lavas of the MA01-02 site, B) Sheeted dykes of the BB01 site, C) Hills of sheeted dykes around the AA01 site, D) Sheeted dykes of the HD01 site.

All paleomagnetic measurements were performed at the Paleomagnetic Laboratory Fort Hoofddijk in Utrecht (The Netherlands). The magnetisation of the samples was measured using a 2G enterprises DC-SQUID cryogenic magnetometer. The bulk magnetic susceptibility (χ_m) was measured for all samples using an Agico supplied MFK1 Kappabridge. For each site, 6 samples were measured using an Agico JR-6A spinner magnetometer for their intensity. All samples were demagnetised using the AF method, and for each site 6 sister samples were demagnetised using the TH method to compare for their results.

In order to demagnetise samples, various components of magnetisation are separated using the relaxation time, coercivity, and temperature in both AF and TH methods (Kirschvink, 1980). It stands for both methods that a grain will more likely carry a secondary magnetisation when the relaxation time is lower (Tauxe et al., 2010). For the AF method, components with a low relaxation time have low coercivities. For the TH method, grains with a lower relaxation time will have low blocking temperatures.

In addition, rock magnetic analysis has been carried out on several samples from pillow lava and sheeted dykes, including thermomagnetic experiments (Curie Balance and susceptibility-versus-temperature), and hysteresis measurements. For several samples the mineralogy was also investigated with optical and Scanning Electron (SEM) microscopy.

3.1 Alternating-Field Demagnetisation

For the AF method, samples were demagnetised using a robotised sample handler (Mullender et al., 2005) that is attached to a horizontal 2G enterprises DC-SQUID cryogenic magnetometer. All samples were inserted in silicon cubes and glued with silicon glue, after which they were automatically demagnetised using alternating magnetic fields in a null magnetic field environment. The peak of the alternating field was incremented using steps of 5-10 mT until a maximum of 100 mT was reached for the samples. With each step, grains, that carry a coercivity slightly lower than the coercivity that the field generates, will save and thus track the field. When the field peak gradually decays below the grains' coercivities, the then current moments will be saved to those grains. Because there is a range of coercivities present in a sample, low stability grains will save the moment first, grains with a higher stability next, and so on. In this way, grains will show magnetic moments along different directions of the alternating field, while the net contribution to the remanence will be zero. The robot AF-demagnetiser tumbles the samples in three directions, so that the samples will be demagnetised around three orthogonal axes.

3.2 Thermal Demagnetisation

Thermal demagnetisation was performed on each site using a magnetically shielded, laboratory-built furnace that has a residual field less than 10 nT, after which their magnetisation was measured using a 2G Enterprises DC-SQUID cryogenic magnetometer. Temperature increments of 50 °C were used until a temperature of 500 °C was reached, after which increments of 20 °C were used. Samples were demagnetised until the magnetic signal was too low (close to zero), or until the magnetic signal showed unstable behaviour. The NRM was measured double-sided by the magnetometer (twice in antipodal positions, after which averaged). In order to minimise the effect of any imparted magnetism that could be obtained by a remnant magnetic field while heating in the oven, samples were arranged in antipodal positions between each heating step when put in the oven.

The TH method uses the varying Curie temperatures in relation to relaxation times of the minerals in a sample. When heated up, grains will be in equilibrium with the field when the relaxation time is a few hundred seconds, reached just below the Curie temperature (unblocking temperature).

3.3 Thermomagnetic and Susceptibility Analysis

In order to describe the main magnetic carriers of the samples, thermomagnetic and susceptibility-versus-temperature analysis was performed on several samples from pillow lava and sheeted dykes. Two devices were used; a house-built horizontal translation-type Curie Balance with a sensitivity of approximately 5×10^{-9} Am^2 (Mullender et al., 1993), and an Agico KLY-3S susceptometer with a CS-3 furnace coupled to it.

For the Curie Balance, approximately 30-80 mg of powdered sample was used per measurement, from both pillow lava and sheeted dykes, and placed into quartz glass sample holders, held in place by quartz wool. Heating and cooling rates were 10 °C per minute. The thermomagnetic run was carried out with several heating steps, with intermittent cooling in between the steps. The successive heating and cooling segments were chosen as follows: 150, 100, 250, 200, 300, 250, 350, 300, 450, 400, 500, 450, 540, 500, 580, and 20 °C.

For the susceptometer, glass tubes were filled with the powdered sample up to a height of approximately 1 cm, sometimes less if the material was too strong. The susceptibility-versus-temperature run was carried out with one big heating step to 700° C.

3.4 Hysteresis Loops and IRM curves

In order to characterise the magnetic domain state of the sheeted dykes and pillow lavas, the saturation magnetisation M_s, the saturation remanent magnetisation M_r, the coercive force B_c and coercivity of remanence B_{cr} of the samples were measured using an alternating gradient magnetometer (MicroMag Model 2900 with 2 Tesla magnet, Princeton Measurements Corporation, noise level 2×10^{-9} Am^2). Hysteresis loops and isothermal remanent magnetisation (IRM) acquisition were measured for 3 to 6 rock chips (1-8 mg) per lithology. The M_s, M_r, and B_c were acquired from these measurements. The field increment is 10 mT and the average time for each measurement 0.15 s.

For the IRM acquisition curves were measured (containing 100 measurements with an initial field of 0.5 mT and final field of 2 T) in logarithmic sweep mode. The back-field demagnetisation curves were measured from this to acquire the B_{cr}.

The ratios M_r/M_s and B_c/B_{cr} were plotted against each other in a Day Plot (Day et al., 1977). The Day Plot helps in distinguishing the different grain fractions in the rock.

3.5 Mineralogy

To identify the minerals and especially to look at the behaviour of magnetite in the samples, thin sections of several sites were investigated with scanning electron microscopy, and also with optical microscopy to a lesser extent. The thin sections have first been coated with platinum, after which they were inspected with a scanning electron microscope (SEM) (model JEOL JCM-6000) in backscatter mode using 15 kV to reveal the microtextures of the magnetic minerals. This gave additional information about the diagenetic conditions and their effect on the magnetic signal.

3.6 Demagnetisation Reliability criteria

After AF and TH demagnetisation, magnetic components in all samples were analysed using Remasoft software (Chadima et al., 2006) after which Fisher statistics (Fisher, 1953) with the 45 cut-off were performed on all the units to determine the averaged direction of magnetisation per site. Graphs were produced with Ghostview and Stereonet8.

Reliability criteria were used after Deenen (Deenen et al., 2011): The radius of the 95% confidence cone (A95) of a site's mean direction for the virtual geomagnetic pole (VGP) should be in between A95min and A95max. When the magnitude of A95 exceeds A95max the data becomes unreliable. When the magnitude of A95 becomes lower than the A95min, the data represents a spot reading, from which we cannot read any paleosecular variation. The radius of the 95% confidence cone for characteristic remanent magnetisation(ChRM), α95, is then set as reliable when smaller than 15°. The Fisher dispersion parameter k for ChRM is set as reliable when bigger than 13, for k (or K) and α95 (or A95) are interrelated according to Butler (1992) and Tauxe et al. (2010). The size of k is dependent on the timespan in which magnetisation took place; when the dispersion parameter k is very large (~100) the result is usually a spot reading (meaning the timespan in which magnetisation took place is rather short), where smaller magnitudes of k (15-30) show secular variation.

The last reliability criterion is the total number of samples for a site, N. A site is accepted as reliable when it contains more than 15 samples, though reliable results can also be contained with a smaller amount of specimens. It is widely accepted that a site should contain at least 7 samples (Tauxe et al., 2010).

4. Results

In this study, the paleomagnetic and mineralogical results of research performed on cores from 12 sites are presented.

4.1 Demagnetisation of the NRM and paleodirections

The samples collected for this study vary much in their magnetic intensities, from the low threshold of 10^{-3} A m^{-1} for many sheeted dyke samples to high intensities of 4 A m^{-1} for some dykes and pillow lavas. Thermal demagnetisation behaviour also appears to show variation between sites, and the magnetisation among samples from the same site also shows a lot of variations (Figure 3). Some sites demagnetise rather quickly, already having lost almost all of their magnetisation at 300 °C and 400 °C (many samples of sites AS, FF, GD, HA) suggesting high titanium-rich titanomagnetite and low content titanomagnetite, whereas most other samples and sites show a much more gradual decay and lose their magnetisation at 580 °C, suggesting that (titano-)magnetite is likely to be the main carrier of the NRM in the samples (MacLeod et al., 2011). Site AA even maintains around 80% of its magnetisation until 580 °C, suggesting that a high-coercivity mineral might be one of the carriers of the NRM in the specimens. From all the samples together, only 10 samples show partial self-reversal, which is very likely caused by alteration.

Most of the samples measured with the AF method show very clear demagnetisation diagrams in a Zijderveld (1967) projection. Typical examples for each site are shown in Figure 3. Samples generally AF demagnetised down to 5-20% of their total NRM when 100 mT was reached, with only one or two samples per site retaining up to 50% of their NRM. Samples measured with the TH method sometimes show more complicated, but still clear demagnetisation diagrams. Many samples in both AF and TH also provided a clear secondary component, or sometimes even a third component, mostly associated with a small present day field overprint. These small overprints were usually removed by 10 mT or 100-150 °C. The *in situ* mean directions of magnetisations are shown in Figure 3 for almost all sites. The only sites not shown, are GD01 and HU01, which didn't go through the 45 cut-off, since these sites were almost completely overprinted by the present day field of Oman (D = 0°, I = 40.3°) and the remaining samples showed a scatter that was too big. For the other sites, the *in situ* directions are significantly different from the present-day field, so these are explained as ancient remanences.

All of the results obtained by Fisher statistics and 45 cut-off can be found in Table 1. Equal area projections are shown in Figure 3 for nearly all sites, showing the mean directions of the ChRM and virtual geomagnetic pole (VGP). The results per site are discussed below and correspond with data from said table.

AA01 – Sheeted dykes – Prior to the 45 cut-off, 11 out of 34 samples were disregarded due to them being situated too close to the present day field (PDF) of Oman. The remaining 23 samples were analysed, and only 1 sample was disregarded by the cut-off. The site passes the Deenen (2011) criteria, and represents secular variation with the dispersion parameter k being 15.4.

AS01 – Sheeted dykes – Ten out of 28 samples were disregarded before the 45 cut-off due to them being too close to the PDF of Oman, or them being situated on the edge of the equal area projection in specimen coordinates, indicating that they were influenced by a paleomagnetic device in the lab or lightning. The remaining samples showed two clusters, out of which one cluster was chosen to be the correct one because in a great circles analysis samples out of the cluster crossed it. The other cluster was rejected for its directions were very likely influenced by a paleomagnetic device in the lab and the PDF. Five samples were then disregarded by the cut-off, giving a total number n of 13. While this is slightly less than the desired 15 samples, the results are still reliable. The remaining samples pass the other Deenen criteria, and while the site shows some scattering in the VGP diagram (Figure 3), the site is still considered reliable.

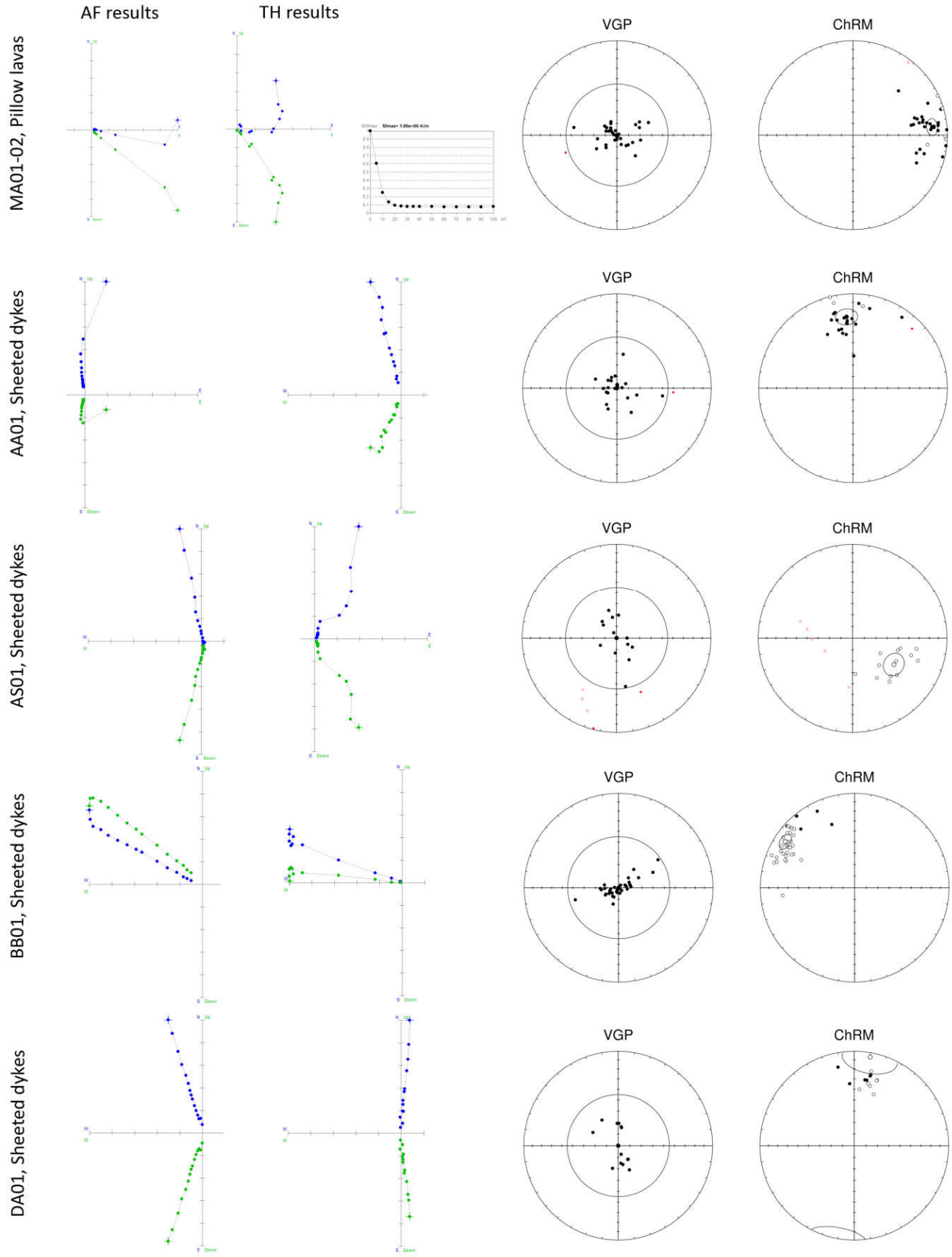

Figure 3(1) Summary of paleomagnetic results from the Oman ophiolite. The first column contains orthogonal vector plots of alternating field demagnetisation for each site (in situ coordinates), the second column contains orthogonal vector plots of thermal demagnetisation for each site (in situ coordinates). Blue/green dots represent the projection of the remanence vector onto the horizontal/vertical plane, respectively. NRM = natural remanent magnetisation. Steps are shown in degrees Celsius or millitesla. The third and fourth columns present equal area projections of specimen mean directions of the ChRM and VGP components, for all sites. The data corresponding with the projections can be found in Table 1.

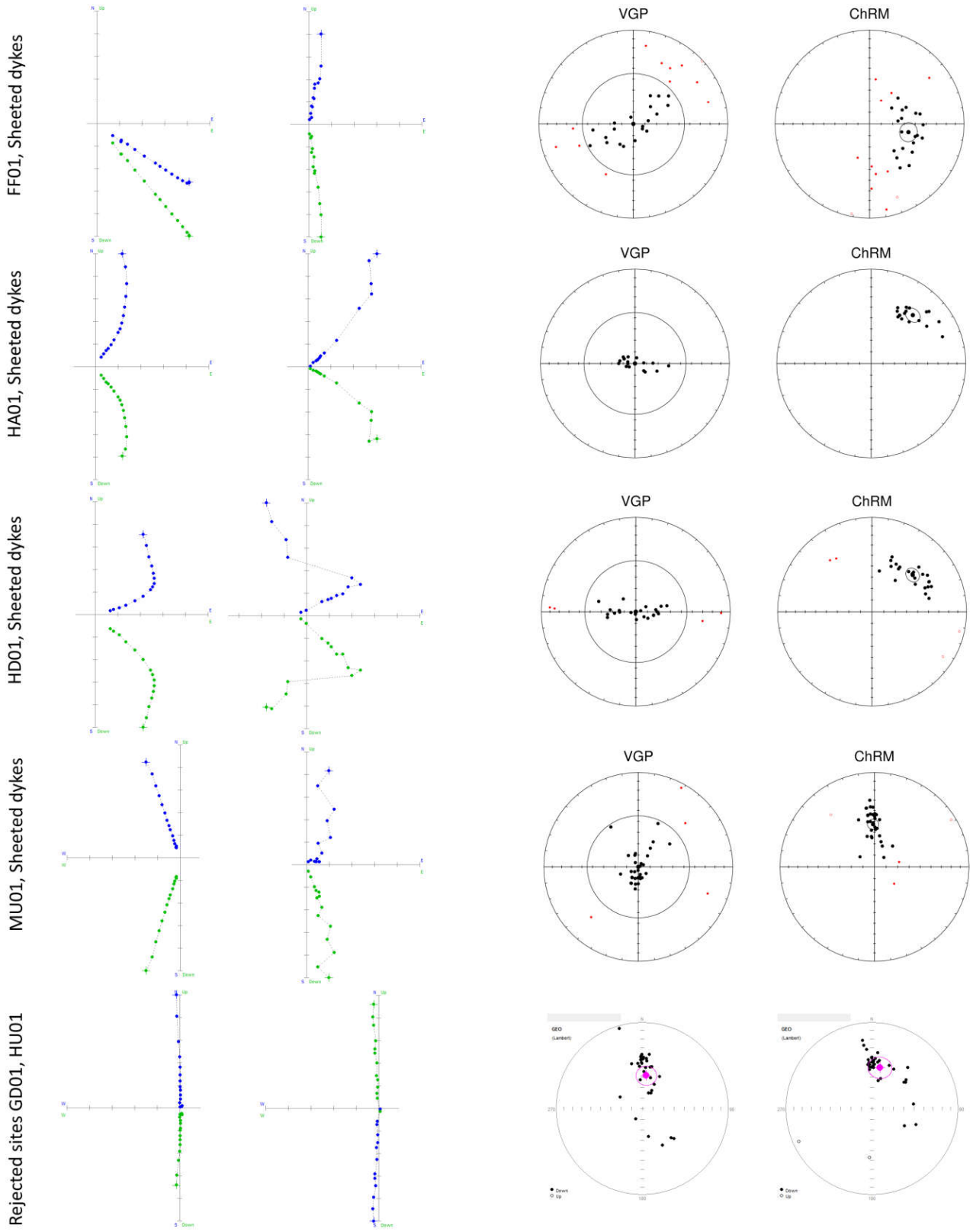
FF01, Sheeted dykes
HA01, Sheeted dykes
HD01, Sheeted dykes
MU01, Sheeted dykes
Rejected sites GD01, HU01
VGP
ChRM
VGP
ChRM
VGP
ChRM
VGP
ChRM
GEO
(Lambert)
GEO
(Lambert)

BB01 – Sheeted dykes – Only one sample out of 36 was removed from this site prior to the cut-off, because it showed a direction in the equal area projection in specimen coordinates that was right in the origin, meaning that an induced direction along the vertical axis of the specimen overprinted the primary signal. This indicates that the sample was drill-induced. No samples were removed by the cut-off, giving a very reliable n of 35. The data of this site is of good quality, with a low α95 of 5.5 and a k of 20.2, meaning the site shows secular variation.

DA01 – Sheeted dykes – Prior to the cut-off, 17 samples out of 30 have been removed from this site due to them showing either drill or machine induced directions in specimen coordinates, and them also representing a PDF. For the remaining samples, none were disregarded during the cut-off, giving a n of 13, which is still considered reliable. The α95 is slightly higher than the desired 15° with 17.8°, and the dispersion parameter k is lower than the desired 13 with 6.4, meaning that the samples are scattered, but the magnitude of A95 lies within its minimum and maximum range, which is why we still consider site DA01 to be reliable.

FF01 – Sheeted dykes – Only three samples out of 35 were disregarded before the cut-off because they didn't show a remanence component that went to zero in a Zijderveld projection (the origin of a Zijderveld projection). In an equal area projection (geological coordinate system) the cluster of samples is shaped elongated with a bend, resulting in 12 samples being disregarded by the 45 cut-off. The remaining samples however (n=20) pass the Deenen criteria, with a A95 of 10.7 in between a minimum and maximum of 3.6 and 12.4 respectively, and a dispersion parameter k of 17.8, which means the site shows secular variation. The site is thus considered reliable.

GD01 – Sheeted dykes – Around 80% of 35 samples of this site showed a clear PDF, or were largely influenced by the PDF. The remaining samples showed no correlation with each other and were largely scattered. The whole site has been disregarded.

HA01 – Sheeted dykes – Before the cut-off, 17 out of 34 samples of this site have been disregarded because they show only a PDF component. The other 17 samples form a cluster which is considered to display the ancient remanence. No samples are disregarded by the cut-off giving an n of 17, and the results pass the Deenen criteria with the magnitude of A95 being in between the minimum and maximum range. With a α95 of 6.1, and a k of 34.9 the site shows secular variation, even though the k is higher than the accepted maximum of 30 for secular variation.

HD01 – Sheeted dykes – Only 4 out of 31 samples were removed prior to cut-off due to them being induced by a paleomagnetic device or struck by lightning. The cut-off disregarded only 4 samples, giving a final n of 23. The data is of a good quality, passing the Deenen criteria with the magnitude of A95 being in between the minimum and maximum range. The site shows secular variation with a α95 of 5.9 and a k of 27.7, and thus was accepted.

HU01 – Sheeted dykes – Around 60% of 35 samples of this site show a clear PDF, and 5 other samples show a drill-induced component. The remaining few samples show a large scattering and no correlation with each other, thus this site has been disregarded.

MU01 – Sheeted dykes – The remanence components of this site seem to be close to the PDF, yet no sample shows a direction that is exactly at the PDF position, unlike sites GD01 and HU01. While the declination of this site (358°) is similar to the PDF, the inclination of the site however is 52.8°, which indicates that this site likely didn't acquire its remanence recently. It might be a coincidence that the average component of this site is close to the PDF, and thus we analyse the site further. After the cut-off 31 of 35 samples are left, and the site passes the Deenen criteria with the magnitude of A95 being in between the minimum and maximum. A k of 31.9, a α95 of 4.6 indicate that the site shows secular variation, even though the k is higher than the accepted 30. We consider this site to be reliable.

MA01-02 – Pillow lavas – While in the field the samples of MA01 and MA02 were sampled to be separate sites, for the analysis we combined them since the samples didn't show two clusters in an equal area plot, but overlapped. Since for half of the samples the remanence component in a Zijderveld projection was hidden due to two overlapping components, we performed a great circle analysis on the site to find the characteristic component. This component should lie somewhere on the great circle, so when we put multiple of them together, their intersection point should fall within the cluster of samples that were analysed by a Zijderveld projection. In the end this provided an inclination of 16.8° (±8.8°) for the pillow lavas, which provides a paleolatitude of 8.6° (±4.8°). The data pass the Deenen criteria with a α95 of 5.9, a k of 19.0, and the magnitude of A95 being in between the minimum and maximum range. Thus this site has been accepted to be reliable.

Sites AS, BB, FF, HA, and HD show an elongated scatter pattern in the VGP diagrams (Figure 3). The reason for this is most likely that the sampled site was long (samples taken over a distance of 30-50 m) which usually results in an elongated distribution, especially if some deformation took place at the location. The elongated pattern however has no influence on the quality or meaning of our data, and doesn't have to be corrected for, since it doesn't change anything about the *in situ* magnetic vector.

It is difficult to say when remanence acquisition took place for each site, but since we excluded the present field overprint, we can at least say the remanence was not acquired recently. The samples taken from the field were also fresh, suggesting that no major metamorphism occurred (further described in section 4.5 – Mineralogy) and that therefore the magnetisation must be primary, and being acquired during the spreading of the seafloor of the Neo-Tethys Ocean.

4.2 Net Tectonic Rotation Results

All net tectonic rotation (NTR) results are listed in Table 2, which is being referred to with 'Preferred solution, Solution 2' etc. Table 2 also lists the average strike and standard deviation for the preferred solution, calculated over 125 iterations. A visual representation of the preferred solution is shown in Figure 10.

In order to put the sheeted dyke sites back to their original frame of reference, NTR analysis is used (Allerton and Vine, 1987; Morris et al., 1998). A reference direction is needed in the analysis which gives a reliable declination and inclination for the location where the ophiolite initially formed. An ad hoc reference direction is adopted using the inclination obtained from pillow lavas of site MA01-02 (16.8° ± 8.8°) and a northern declination (000°/16.8°).

This reference direction has been used on all the sites listed in this study.

NTR analysis rotates sheeted dykes back to the reference direction and to its original vertical position at the same time, calculating two solutions for one input, as can be seen in Table 2. To determine which of the solutions is preferred, the most reliable solution was chosen on the basis of reliability criteria according to Allerton and Vine (1997) and Morris et al. (1998). Mainly the component of tilt and the direction of the rotation axis were used as a reliability criterion in this study, combined with the information received from geological maps. For example, more tilt is expected in zones surrounded by faults, and less tilt expected in zones without any nearby faults.

It has to be taken in mind that above reliability criteria are not purely based on mathematics, but on logics instead, and that they therefore only give a possible preferred solution. It also has to be taken in mind that the rotations given by the NTR program are absolute rotations without a given timespan, and thus that anything can happen in between the initial and final dyke orientation.

MA01-02 – Pillow lavas – The pillow lavas of Oman are known to be quite well-preserved, and for site MA01-02 in the Sarami Block their direction could be well recognised in the field, also with the help of some lava flows. By a simple tilt correction on the pillow lavas a corrected paleomagnetic direction of 084.2° (±4.8°) / 16.8° (±8.8°) was obtained. This indicates an absolute rotation of 84.2° clockwise (CW) and paleolatitude of 8.6° (±4.8°), which is consistent with other large rotations found for the Oman pillow lavas, like a 145-150° rotation found by Perrin et al., (1994, 2000).

When we assume that the Sarami block didn't undergo any significant internal deformation, we can adopt the tilt-corrected direction as a reference direction for the NTR analysis for the sheeted dykes of Oman.

AA01 – Sheeted dykes – In the field, for these sheeted dykes a structural direction of 345°/70° was found, and in the lab an in situ mean direction of 355°/25° was measured. NTR analysis gives two results, of which one with a 26° counter-clockwise (CCW) rotation around a 019°/30° rotation pole, and the other with a 156° CW rotation around a 357°/20° rotation pole. In both cases, the initial dyke orientation is striking N-S, with 180° for one solution, and 000° for the other. For the solution with the large 156° CW rotation, the rotation pole is very shallow and pointing North, which would give a complete turnover of the whole sheeted dyke. This doesn't make sense when compared with the geological map (Figure 9) that shows an E-W striking thrust fault just a few kilometres south of the site, perpendicular on the rotation axis. The other solution shows a much simpler solution, only slightly tilting the sheeted dyke in CCW direction, which makes much more sense. Therefore we accept this as our preferred solution.

AS01 – Sheeted dykes – The sheeted dykes of AS01 were sampled stratigraphically just below the pillow lavas of site MA01-02. Their measured structural direction is 145°/40° with an in situ mean direction of 123°/-47° obtained in the lab. The two rotation solutions given in the NTR analysis both show a CW rotation, of 145° with a pole of 187°/51° and of 133° with a pole of 079°/15° respectively. The last named solution would completely overturn the sheeted dykes with its very shallow rotation axis, which does not make sense with what we saw in the field; the pillow lavas directly on top of these sheeted dykes were not overturned. The preferred solution makes much more sense in that it doesn't overturn the ophiolites, and its large CW rotation would also make sense considering the large CW rotation found in the pillow lavas. This solution places the sheeted dykes in an initial 157°/90° orientation.

BB01 – Sheeted dykes – The measured structural direction in the field of the BB01 sheeted dykes is 103°/77° with an in situ mean direction of 304°/-13° found in the lab. The rotation poles of the two given solutions are fairly different; 204°/55° with a CCW rotation of 67° and 331°/05° with a CW or CCW rotation of 172°. We disregard the latter solution directly, for it would rotate the sheeted dykes around a very shallow axis with a large amount of rotation, and the axis would be perpendicular on a fault system found 7 kilometres from the site with an NE-SW strike (Figure 9). The other solution makes great sense, with a steeper rotation pole and a smaller amount of rotation, the rotation axis being parallel to found faults. The obtained initial dyke orientation for this solution is 163°/90°.

DA01 – Sheeted dykes – Sheeted dykes of site DA01 were measured in the field to have a structural direction of 358°/38°, and an in situ mean magnetic direction of 010°/-05°. The two solutions given by the NTR analysis are only different in that their rotation pole has a slightly different orientation, and that for one solution the rotation angle is twice as big as for the other solution, but they both rotate around a very shallow rotation pole; 163°/04° with a 53° CW rotation and 011°/08° with a 127° CW rotation. We chose for the former solution, because it shows a more simple rotation, and because it places the sheeted dykes dipping to the east while placing the bedding dipping to the west, which makes sense with the nearby bedding (Figure 9). This gives an initial dyke orientation of 169°/90°.

FF01 – Sheeted dykes – For site FF01 a structural direction of 165°/53° was measured in the field, and an in situ magnetic mean direction of 102°/55° in the lab. The two solutions given by the NTR analysis are different; 248°/11° with a CW rotation of 88° and 315°/65° with a CW rotation of 103°. The former solution would slightly overturn the sheeted dykes and provide vertical bedding, while the latter solution gives it a slight tilt to the east. This makes much more sense with the pillow lavas and cherts found directly on top of these sheeted dykes a kilometre to the NE (Figure 9), and thus this was accepted as our preferred solution. The initial dyke orientation is 071°/90°.

HA01 – Sheeted dykes – The sheeted dykes of site HA01 have a structural direction of 295°/47° and an in situ magnetic mean direction of 041°/33°. Lava flows are found directly on top of the sheeted dykes to the east. The two solutions given by the NTR analysis give two different rotations; 028°/07° with a CCW rotation of 88° or 009°/42° with a CW rotation of 98°. The former solution does not make sense, because it would emplace the lava flows on the west side of the sheeted dykes in a vertical orientation. The latter solution makes more sense, because it would tilt the sheeted dykes slightly overturned dipping to the NE,

which makes sense with the lava flows to the east of the sheeted dykes dipping towards the SW (which means they would also be overturned) (Figure 9). The CW direction of rotation also makes more sense than a CCW rotation, since site HA01 is situated fairly close to the pillow lavas of site MA01-02, which also showed a CW rotation. The initial dyke orientation is 014°/90°.

HD01 – Sheeted dykes – The structural direction of the HD01 sheeted dykes found in the field is 006°/65° and the in situ mean magnetic direction found in the lab is 048°/42°. The two obtained solutions from NTR analysis vary in rotation angle a lot; 236°/27° with a 51° CW rotation and 018°/36° with a 157° CW rotation. The former solution tilts the sheeted dykes to the NW, the latter solution slightly overturns the sheeted dykes and makes them E-W trending with a steep southward dip. From the geological map (Figure 9) we find that HD01 is situated in a syncline with N-S oriented thrust faults; therefore the sheeted dykes tilting NW sounds reasonable, but an E-W trending overturn with southward tilt wouldn't make sense. Therefore we accept the former solution as our preferred solution, placing the dyke in an initial 171°/90° orientation.

MU01 – Sheeted dykes – The sheeted dykes of site MU01 have a structural direction of 182°/34° and an in situ magnetic mean direction of 358°/53°. The two solutions given by the NTR analysis vary a lot in the amount of rotation and the direction of the rotation pole; 326°/28° with a 66° CW rotation and 005°/35° with a 154° CCW rotation. The former solution tilts the sheeted dykes to a NW-SE trending position, dipping shallowly to the SW; the latter solution overturns the sheeted dykes, overturning the overlying bedding as well. The latter solution does not make sense with the pillow lavas that lie directly on top of the sheeted dykes, just a kilometre to the east (Figure 9), which show similar directions to the nearby pillow lavas of site MA01-02 that were not overturned. The latter solution also shows a big CCW rotation, which does not make sense with the CW rotation of site MA01-02. The former solution is much simpler, and tilts the sheeted dykes and bedding to an orientation consistent with what was found in the field, and seen on the geological map. This is accepted as our preferred solution, and gives the dykes an initial orientation of 139°/90°.

4.3 Thermomagnetic analysis

From the rock magnetic analysis we can say something about the main carriers of the magnetism in the sheeted dykes and pillow lavas. Figures 4 and 5 show the results for both sheeted dyke sites and pillow lavas. For the magnetisation-versus-temperature measurements done with the Curie Balance the diagrams show that (titano-)magnetite is the main carrier of both sheeted dykes and pillow lavas, with unblocking temperatures between 540° and 580° C. The diagram of BB0127 looks like it hasn't reached the unblocking temperature yet, and it looks like maybe hematite or new formed maghemite might be a carrier of the magnetism here. From the susceptibility-versus-temperature measurements we that (titano-)magnetite is the main carrier of magnetism.

4.4 Hysteresis loops and Day Plot

Hysteresis results reveal pseudo-single-domain behaviour for both the sheeted dykes of site AA01 and pillow lavas of site MA01-02 (Figures 6 and 7). The hysteresis loops are open, and are all saturated at 500 mT. The Mr/Ms ratios variate from 0.18 to 0.22 and the Bcr/Bc ratios from 1.89 to 2.72. The Bc and Bcr values are low, indicating a dominant low-coercivity component. The Mr/Ms ratio of 0.18-0.22 correspond with grain sizes of 5-8 µm (Tauxe, 2010).

4.5 Mineralogy – Microscopy Analysis

Several sheeted dyke sites were observed in plane polarised light (PPL) and cross polarised light (XPL) microscopy. There are no representative images of the observations, but we present the main results nonetheless.

Sheeted dykes – Sites AS01, AA01, DA01, FF01, HU01, MU01 – For all the sheeted dyke thin sections, the composition consisted of mainly plagioclase, (clino)pyroxene, and magnetite.

AA01 contains very large magnetite crystals, indicating that they might be multidomain, and a matrix of elongated plagioclase and both clino- and orthopyroxene crystals. Around 5% of high-relief olivine crystals are found, as well as 5% chlorite/premite, and no sulphides. The thin section of HU01 shows the same composition as AA01.

FF01 contains only 5% magnetite, and the matrix, consisting of 70% plagioclase and clinopyroxene, is isotropic. It seems like the magnetite is either growing around chlorite crystals (which contained iron), or the chlorite growing around the magnetite. The chlorite grew at the expense of pyroxene, where pyroxene patches have all been destroyed and cannot be seen anymore. For our results, it doesn't matter whether the magnetite grew around the chlorite crystals or vice versa, because the magnetite crystals are multisegment, delivering a good magnetic signal. Just like for FF01, also in AS01 the magnetite follows clusters of chlorite (or vice versa). AS01 contains more clinopyroxene and less plagioclase than FF01.

Composition-wise, DA01 and MU01 are similar to AS01, both isotropic, without the magnetite following chlorite clusters. Magnetite crystals in DA01 are the smallest from all observed thin sections.

Pillow lavas – MA01 – The pillow lavas of MA01 contain lots of large yellow-orange (PPL and XPL) crystals that do not show extinction or cleavage; they have been interpreted as iron sulphides,. The matrix of MA01 is weathered (pyroxene) and isotropic, where the plagioclase is still fresh. The magnetite crystals appear to be weathered.

4.6 Mineralogy – SEM Analysis

Images taken with the SEM microscope are shown in Figure 8 for each studied site. The grain sizes per site vary a lot, especially for magnetite. For the SEM analysis we mainly looked at the distribution of ferromagnetic minerals (random or aligned), the overall size of magnetite (both multidomain and singledomain crystals), the shapes of crystals, and the composition of the sites. Details per site are given below.

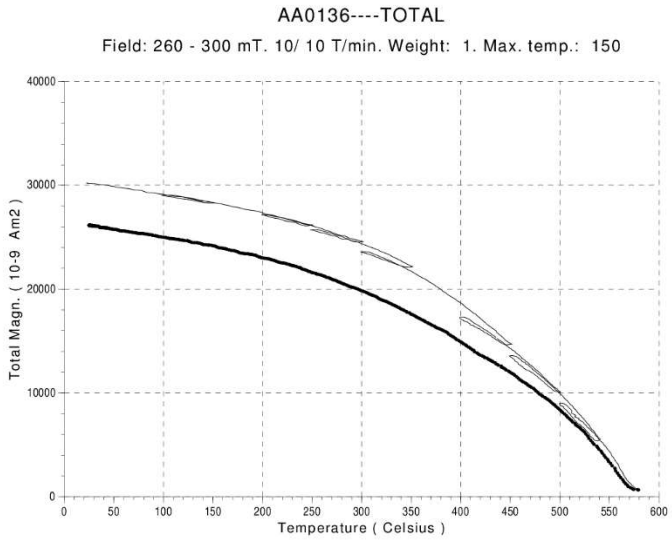

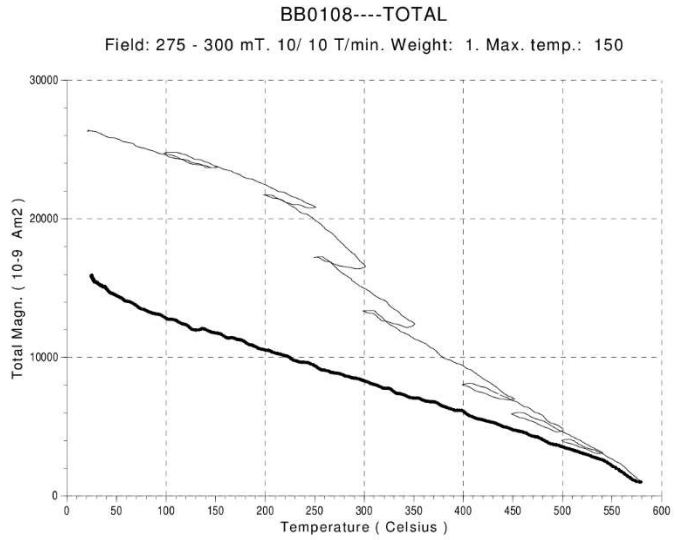

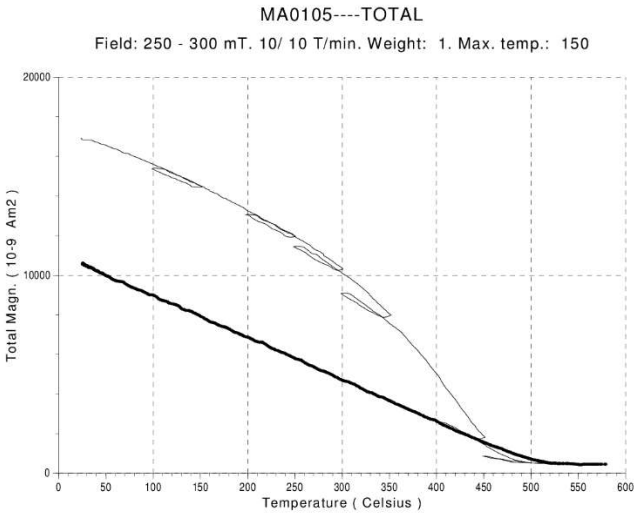

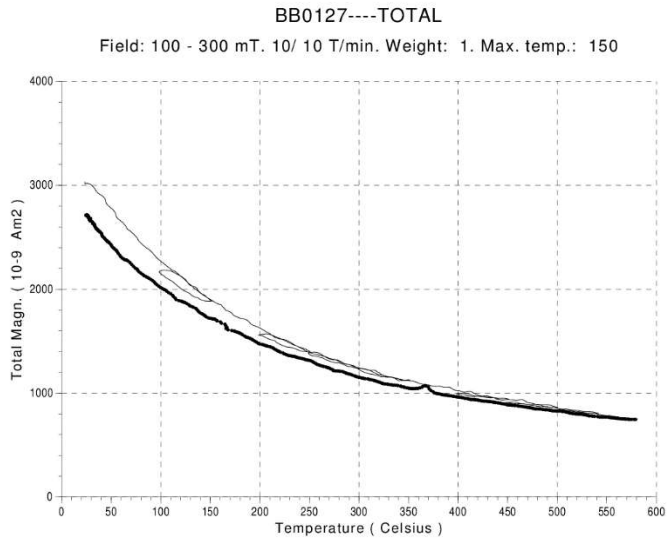

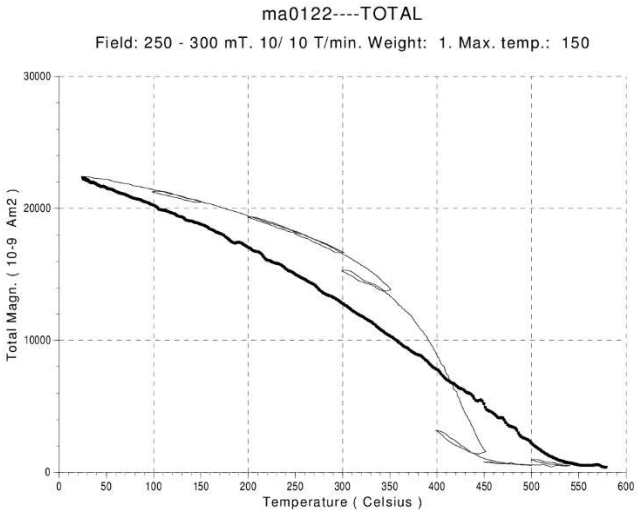

Figure 4. Typical rock magnetic results for magnetisation versus temperature from sheeted dykes and pillow lavas.

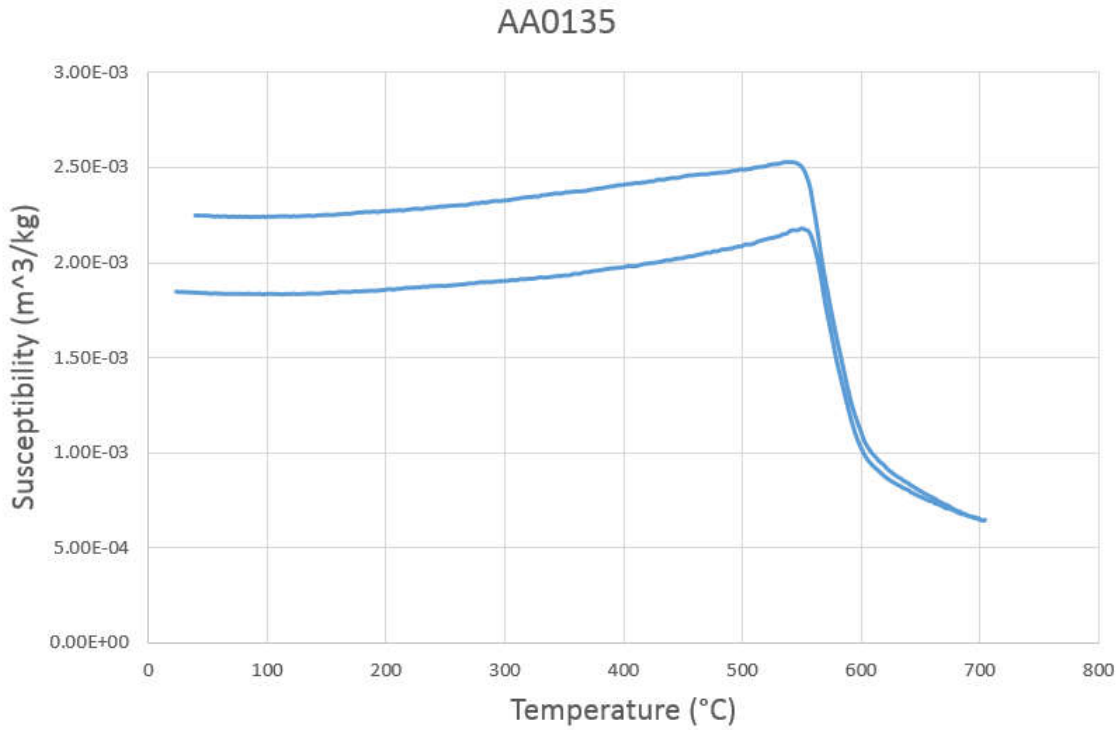

Figure 5. Typical rock magnetic result for susceptibility versus temperature from sheeted dyke site AA01.

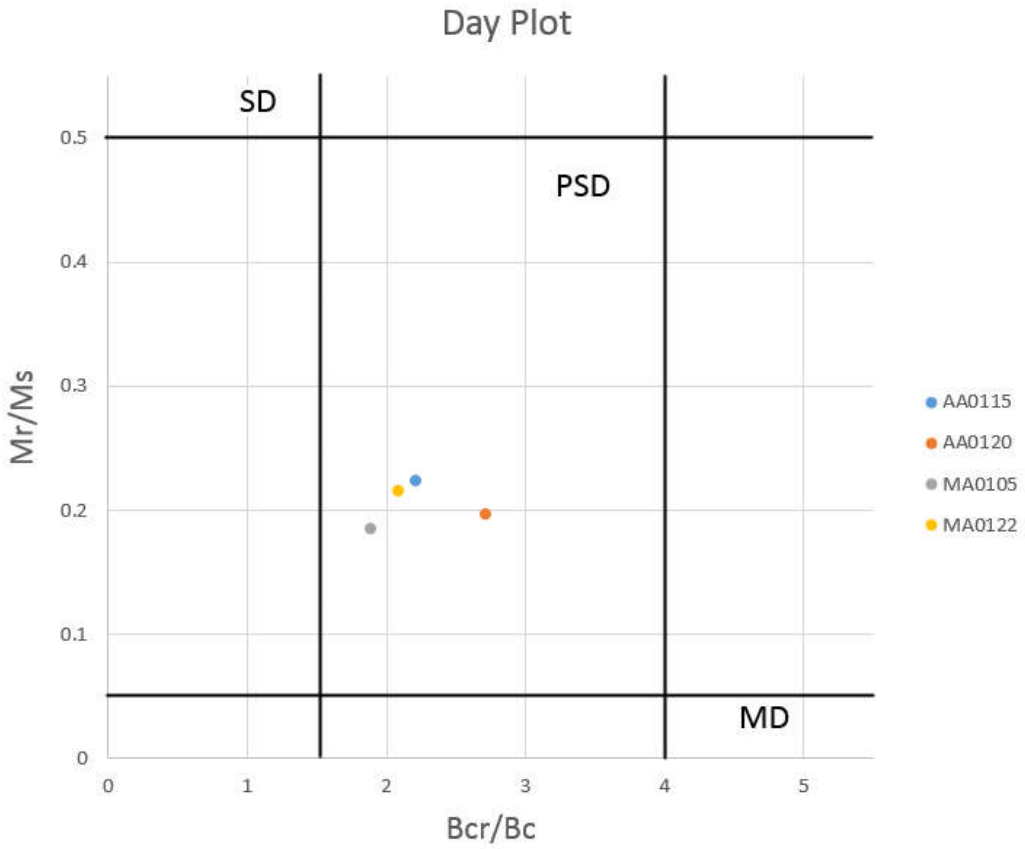

Figure 7. Day plot for AA01 sheeted dykes and MA01 pillow lavas.

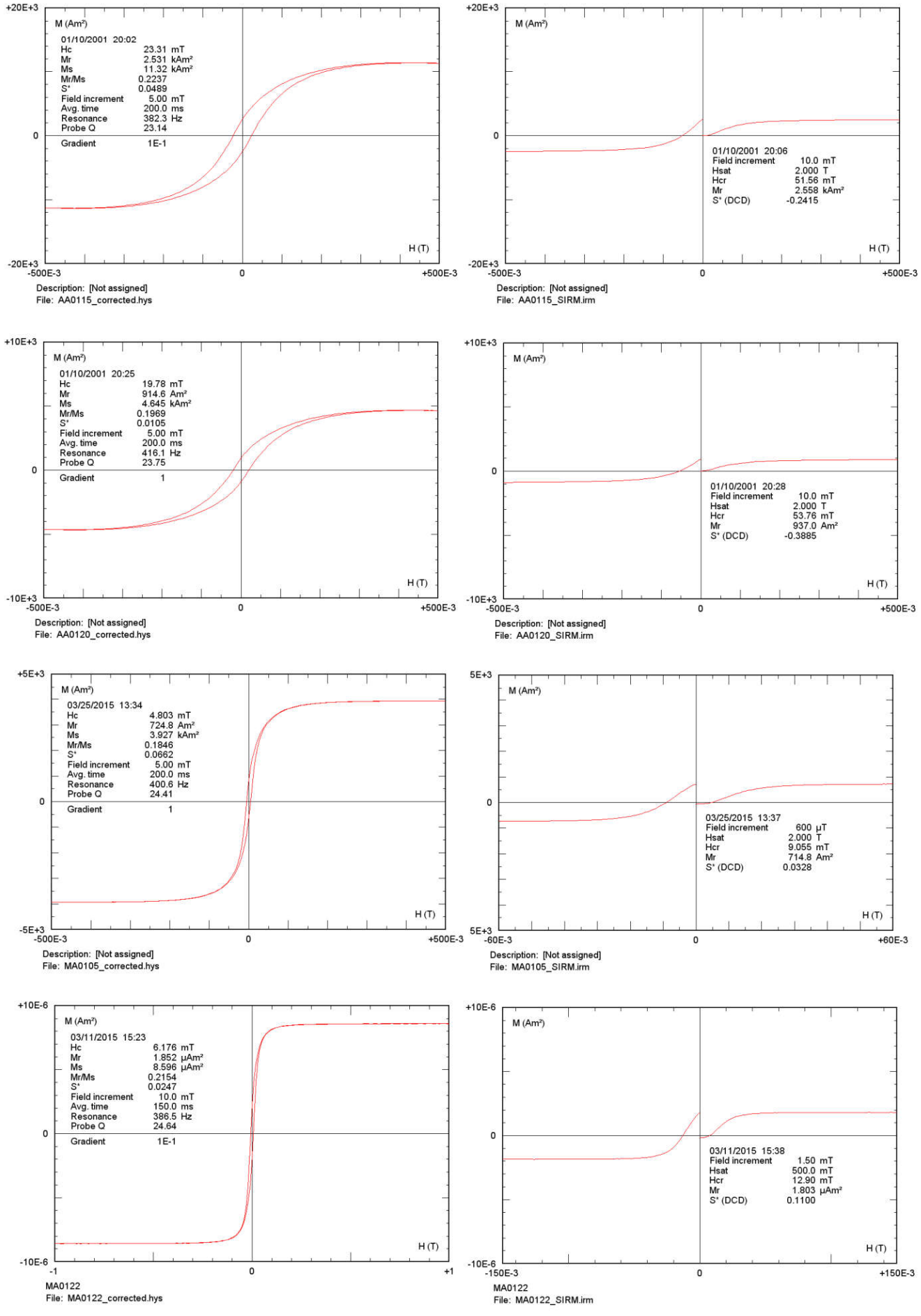

Figure 6. Typical rock magnetic results obtained with hysteresis loops from sheeted dykes and pillow lavas.

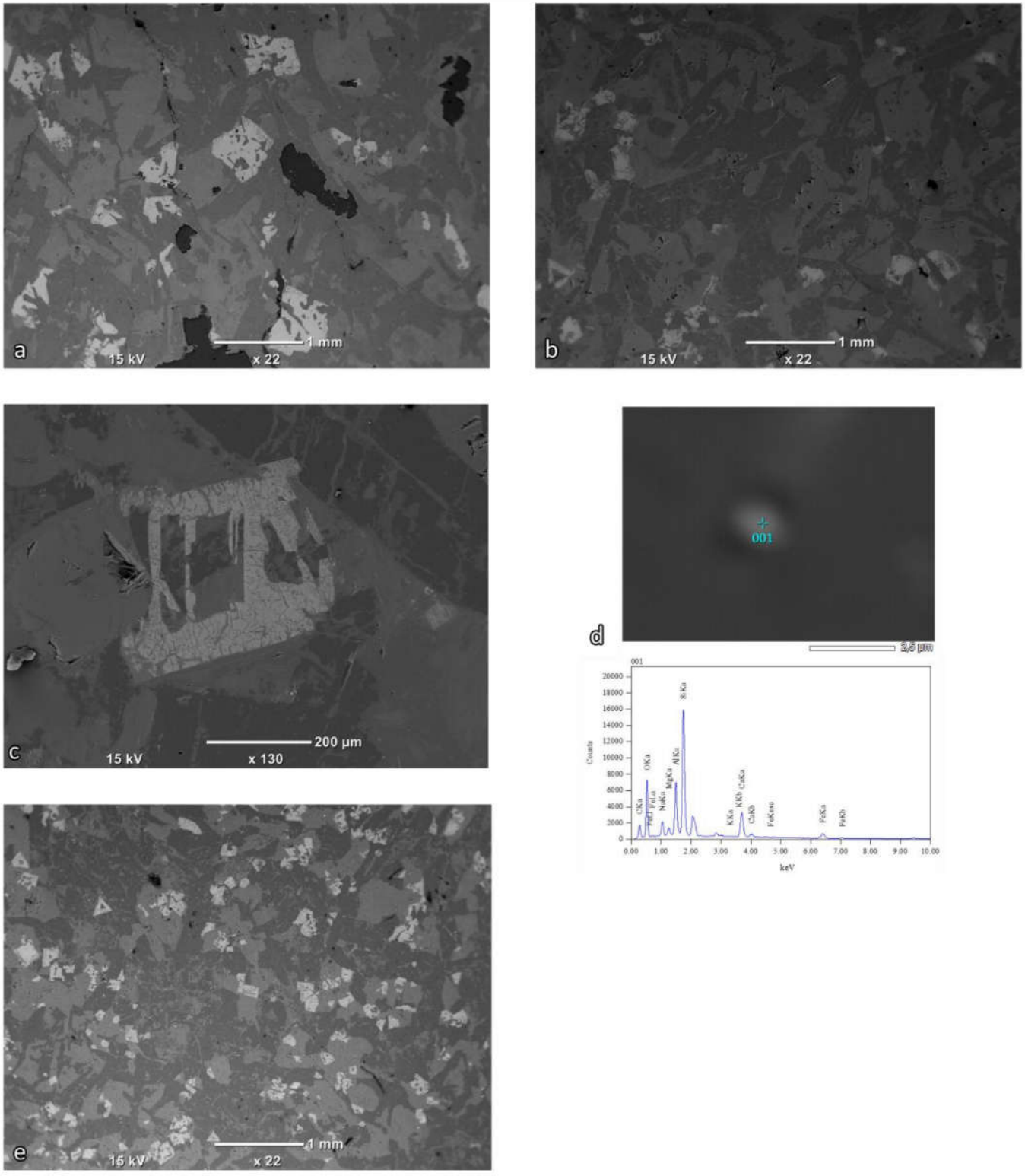

Figure 8. Scanning electron microscope images of thin sections, showing a variety of observed behaviours. D and H also contain compositional diagrams for single domain magnetite.

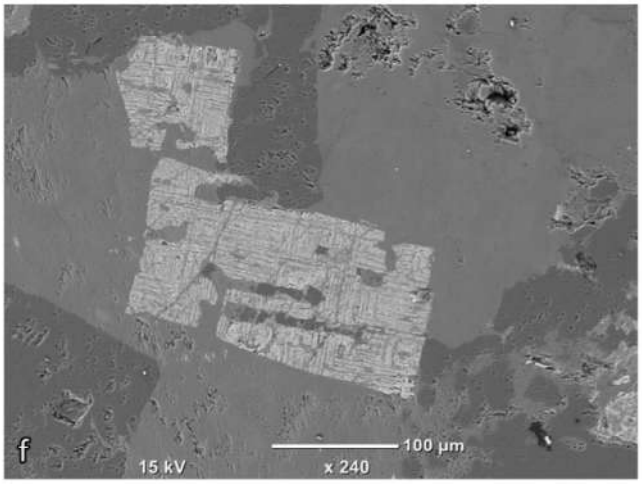
f
15 kV
100 µm
x 240

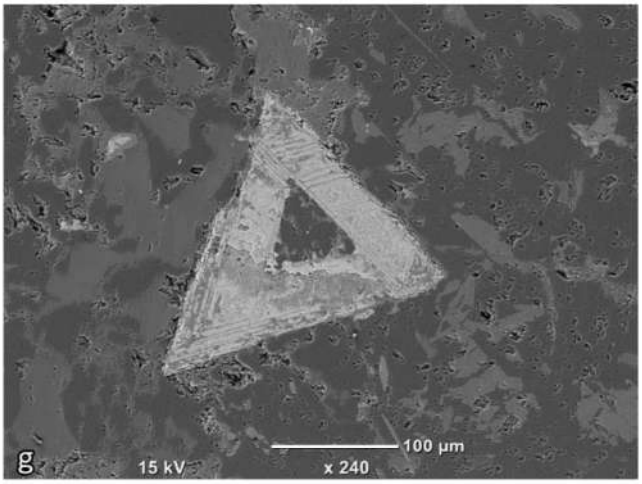
g
15 kV
100 µm
x 240

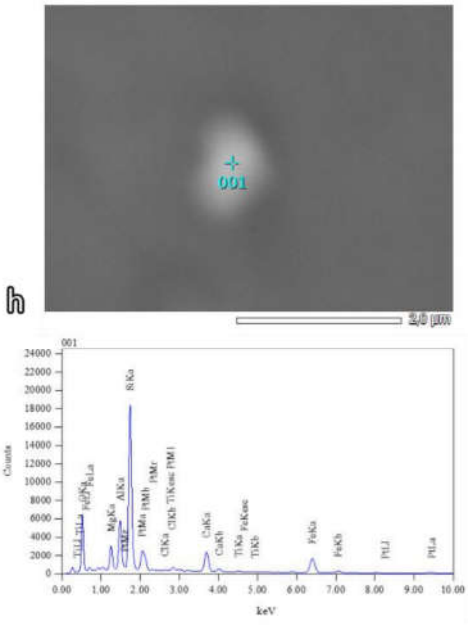
h
001
001
Counts
keV
Si Ka
Al Ka
Mg Ka
Ca Ka
Ti Ka
Fe Ka

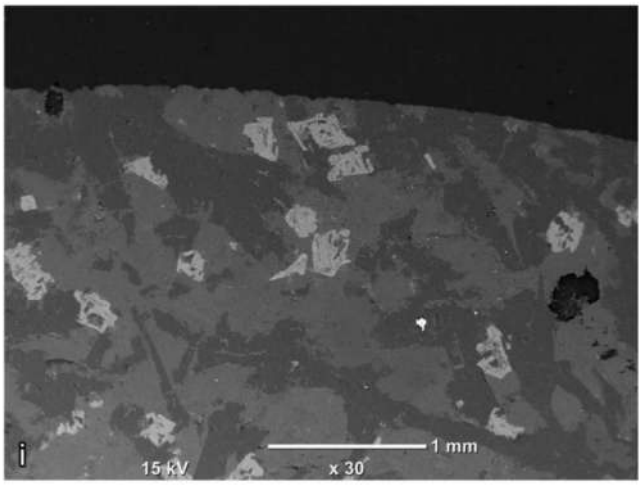
i
15 kV
1 mm
x 30

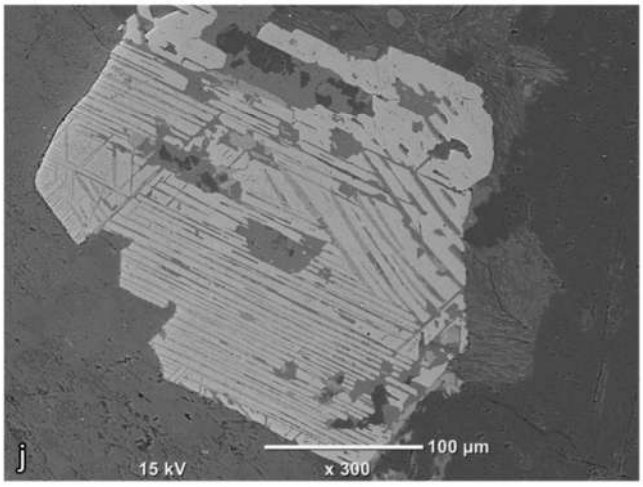
j
15 kV
100 µm
x 300

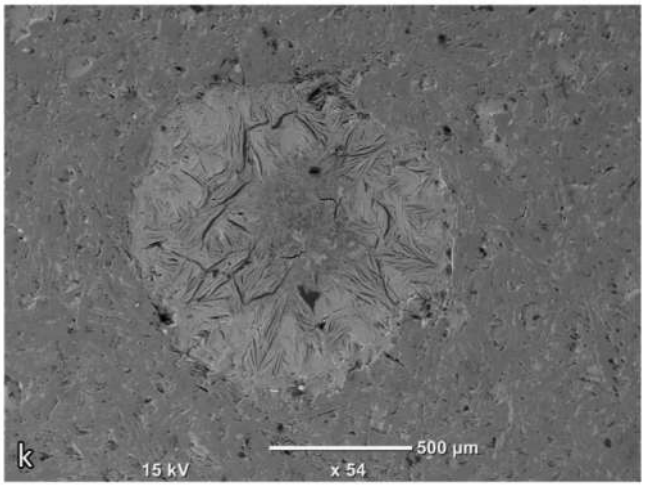
k
15 kV
500 µm
x 54

AA01 – Sheeted dykes – The titanomagnetite of the sheeted dykes of AA01 seems to be randomly distributed (Figure 8 A) and appears to have a very blocky shape. Most of the magnetite crystals are big, ranging from 0.1 mm to 0.8 mm in size (some even visible by the naked eye).

AS01 – Sheeted dykes – The sheeted dykes of AS01 contain big magnetite crystals that are 0.1 to 0.5 mm in size (Figure 8 B). They are not randomly distributed, but are found against chlorite crystals. They also formed or grew at a later stage than the matrix, for they have grown on top of the plagioclase and pyroxene (Figure 8 C). The magnetite crystals of these sheeted dykes do not contain titanium, and also contain only a small amount of magnesium. The sheeted dykes do contain single domain magnetite (Figure 8 D).

FF01 – Sheeted dykes – The titanomagnetite of the sheeted dykes of FF01 is not randomly distributed, but is found around chlorite (Figure 8 E). The big, multidomain magnetite crystals have a blocky shape, some of them even being rectangular or triangular, and show compositional bands that are 90° perpendicular on each other (Figure 8 F and G). This zonation, or banding, is caused by exsolution of titanium; when the titanomagnetite was formed, the rock had a high titanium content, and during temperature drops the system fell into two phases, causing the precipitation of titanium. The black bands therefore consist of rutile, and the white bands of low content titanomagnetite. Single domain crystals of magnetite were also found in this sample, shown in Figure 8 H.

HU01 – Sheeted dykes – The sheeted dykes of HU01 contain magnetite crystals that are 0.05 to 0.4 mm in diameter and take up 5% of the total composition. The crystals are randomly distributed and show a blocky shape (Figure 8 I), also containing compositional bands (Figure 8 J).

MA01 – Pillow lavas – The pillow lavas of MA01 contain a very weathered matrix with possibly big weathered magnetite crystals randomly distributed in it (Figure 8 K). It is not clear if the zonation was caused by precipitation of titanium, or caused by weathering. The matrix consists of pyroxene that seems to be very weathered, and plagioclase that still seems to be fresh.

5 Discussion

In this section the results obtained in this study will be discussed and the main question formulated in the introduction will be addressed; What was the paleodirection of spreading of the Oman ophiolite? The results are interpreted and hypotheses for possible tectonic models are made for the evolution of the Oman ophiolites.

5.1 Reliability of data – Rock magnetic analysis

From the results obtained by rock magnetic analysis, we can say that the data obtained from the sheeted dykes is reliable and can be used to obtain the paleospreading direction of the whole ophiolite. Primary magnetisation was found in multiple samples in the form of single domain magnetite (SEM), and from the pillow lavas it can be said that the site is completely pseudo single domain (Day Plot). Magnetite was found to be the main carrier of magnetisation in the sheeted dykes and pillow lavas.

The *in situ* mean magnetic vector obtained from site AA01 dips shallowly in a NNW direction (355°/25°). The same direction was found by Feinberg *et al.*, (1999) and explained by them as a remagnetised direction obtained by serpentinisation from the upward metamorphic fluid advection in the faulted ophiolite. We didn't disregard the data of this site however, since we didn't find any evidence at the location of site AA01 of serpentinisation, and no veins were found at the site. No sulphides were found either in PPL/XPL and SEM microscopy. From the results obtained from the Day Plot, we also believe that at least part of the magnetisation in this site is primary, since its samples show pseudo single domain behaviour. In addition, the results for site AA01 obtained with NTR analysis give an initial dyke orientation for the sheeted dykes that is consistent with the other sheeted dykes, and its sense of rotation is consistent with the nearby sheeted dyke site BB01.

5.2 Paleolatitude and rotation

The paleolatitude of spreading of the Oman ophiolites was determined by the pillow lavas of site MA01-02, which provided a tilt corrected paleomagnetic direction of 084°/16.8°. This corresponds with a 84° CW rotation for the pillow lavas, and a paleolatitude of 8.6° (±4.8°)N at the time of magnetisation acquisition that happened at 91 Ma. A similar paleolatitude was found by Thomas et al., (1987) between 0-10°N at an age of 80 Ma. Perrin et al., (1994) found an even bigger CW rotation of 145-150° corresponding with a similar initial paleolatitude of 10° N, and found varying rotations for lava flows that formed at a different time; thus the differential rotation must have happened during an extension phase. While we do find large rotations in the pillow lavas that seem to be accurate, we don't find these large rotations in the sheeted dykes directly below the pillow lavas, indicating that local tectonic rotation has taken place in between these lithologies, likely during times of extension. This rotation doesn't change the inclination of the site, so the inclination can still be used for the paleolatitude.

5.3 Paleodirection of spreading

It is widely accepted that dykes intrude vertically and parallel to the axis of the spreading ridge (Pozzi et al., 1984). This can be observed in modern spreading systems, like in Iceland, the Asal rift in Afar, or in the rift valleys of active ridges (Pozzi et al., 1984). This is why in this study we use the orientation of the Oman sheeted dyke complexes to infer the paleodirection of spreading. Summaries of the interpretation of the results can be found in Figure 10, which shows the initial dyke orientations found at each site plus the rotations, and thus also the ridge spreading directions. A Rose diagram of all calculated iteration solutions (875 total) for the N-S striking sites is shown in Figure 11 to illustrate the initial dyke orientation. The total average that was derived from the initial N-S striking dykes was found to be 166.9° with a standard deviation of 21.3°.

The sheeted dykes of the Oman ophiolite show a consistent orientation both for their present day orientation and their initial orientation, seen in Figure 1 and Figure 10 respectively. In general the present day dyke orientations follow the strike of the nappe, except for at the edge of the nappe where sheeted dyke complexes are found that are perpendicular to the strike of the nappe (Nicholas et al., 2000). The initial dyke orientations show a general NNW-SSE orientation with a CW sense of rotation in the North and Central blocks of the nappe, and a CCW sense of rotation in the Eastern block of the nappe. One site of exception is

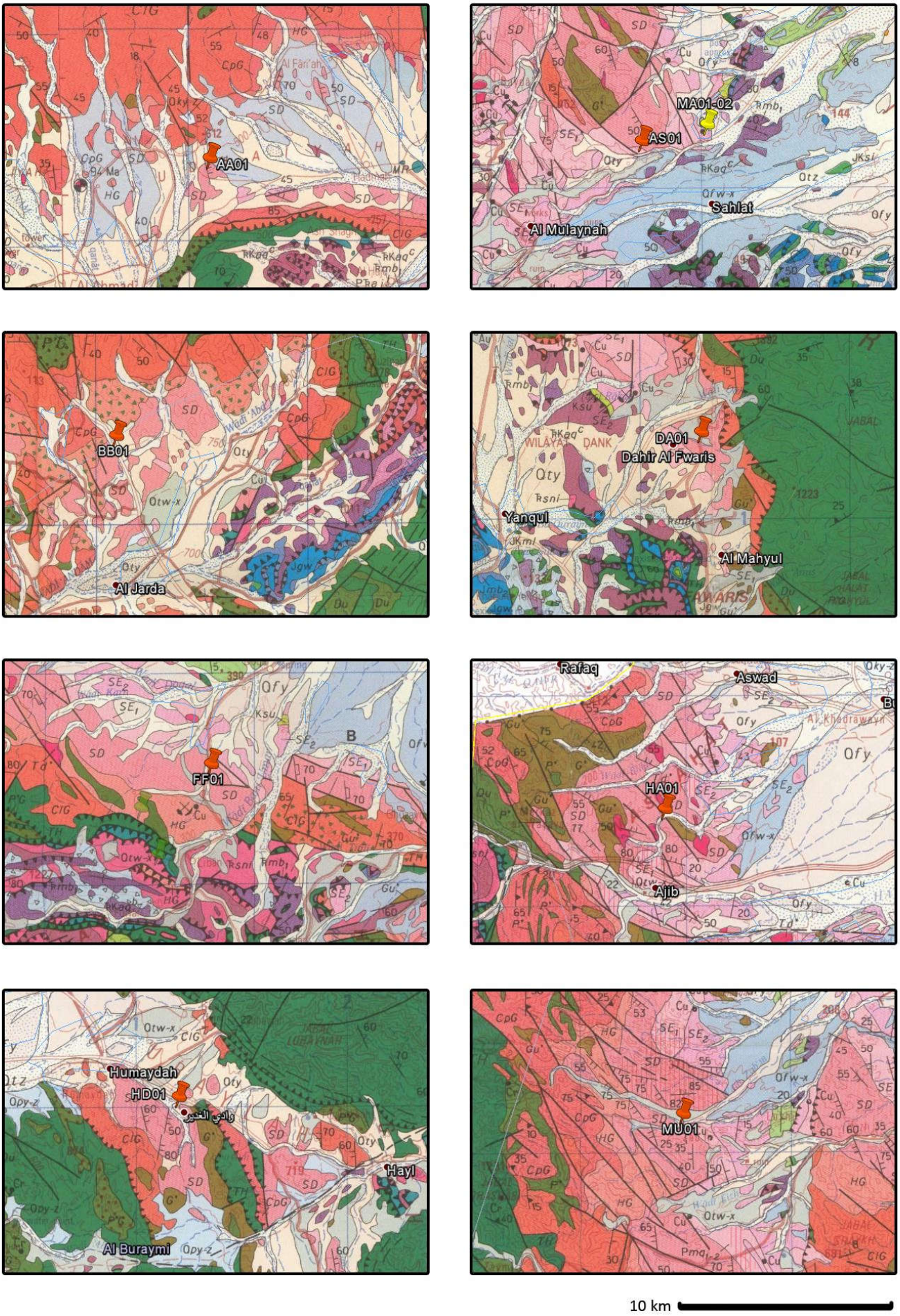

Figure 9. All sheeted dykes in geological context.

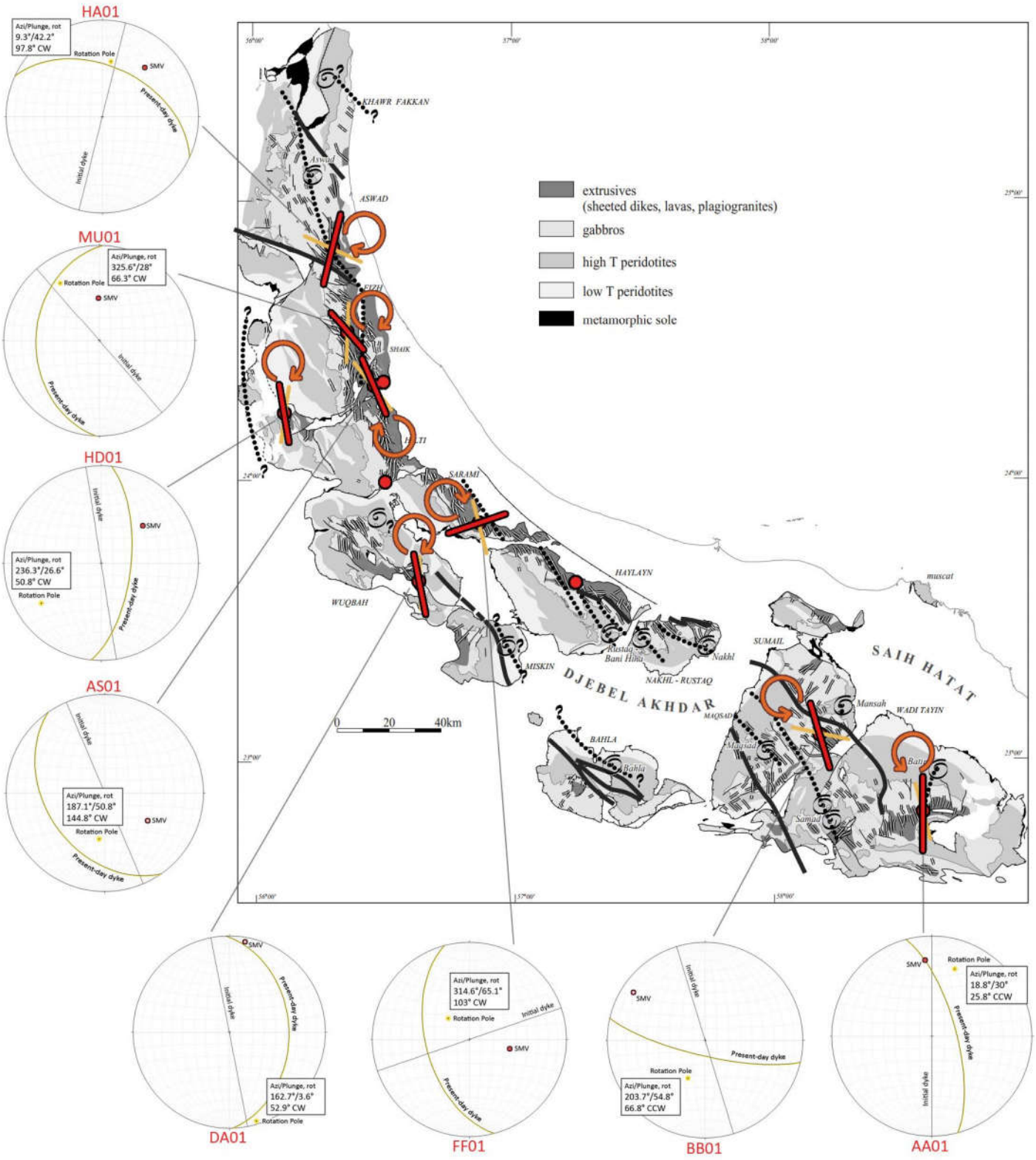

Figure 10. A summarising map showing the ridge orientations per site, as well as the rotation poles and angles in stereoplots. Red lines represent the initial dyke orientation, yellow lines represent the present-day dyke orientation, and orange arrows represent the sense of rotation (CW or CCW). The map was modified from Nicolas et al., 2000.

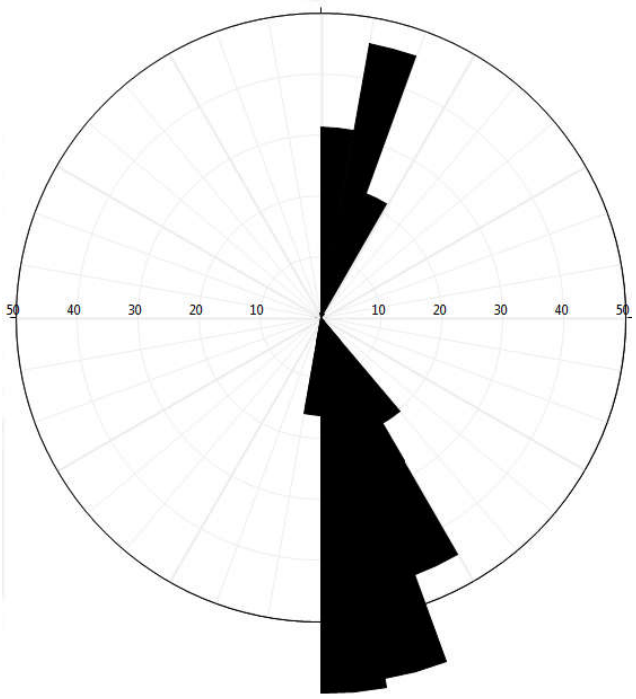

Figure 11. Rose diagram for sites AA, AS, BB, DA, HA, HD, MU, including a total of 875 initial dyke solutions calculated with NTR iteration.

site FF01 that shows an ENE-SWS initial dyke orientation. This will be discussed later.

From these data we can consider that the paleospreading ridge was roughly N-S oriented for the Oman ophiolite, and that the direction of spreading thus was in an E-W direction, considering that the direction of spreading is perpendicular to the ridge orientation.

5.4 Geodynamics of spreading and the evolution of the Oman ophiolites.

Authors have proposed in the past that the Oman ophiolite had been formed along a spreading ridge in the middle of the Neo-Tethys Ocean. Some say that thrusting and subduction initiated the forming of the ophiolite at the Neotethyan ridge (Nicolas, 1989), some assume that the ophiolite formed in a supra-subduction back-arc context in the Neo-Tethys Ocean (Lippard et al., 1986). We propose that the Oman ophiolite did not form in the Neo-Tethys Ocean., because we find an initial N-S orientation of the paleospreading ridge.

Gaina et al., (2015) state that the NW India, Waziristan (Pakistan), and Masirah (Oman) ophiolite result from relative motions between India-Africa and Arabia. We propose that the Oman ophiolite can also be formed by the same plate motions. Between 133 Ma and 90 Ma, the Indian continent broke loose from the African continent to start drifting in a NE direction, during which India rotated in a CCW sense around a rotation pole north of the continent. Transform faults were found during this time north of the continent, oriented roughly N-S, with E-W oriented spreading ridges in between (Figure 12 a). South of the Indian rotation pole, roughly N-S oriented transform movements are converted into extension when India moves and rotates away from Madagascar (Figure 12 a and b), possibly caused by mantle plume activity (Moromdova plume, Gaina et al., 2015). To the North of the rotation pole, this leads to compression in an E-W direction, which causes the Waziristan ophiolite to obduct upon the Indian continent. This happened around 96-91 Ma, as found by the age of the Waziristan ophiolite by Robinson et al., (2000), which happens to be the same age of the Oman ophiolite. Because of the E-W compression to the North of the rotation pole, subduction initiation takes place along the transform faults, and newly oriented spreading ridges with a N-S orientation are formed (Figure 12 c). Subduction zones are found over the world in the direction of absolute plate motion. The plate motion of the Indian continent follows a course to the NE, and because of this motion the once N-S oriented subduction zone rotates into an easier NW-SE orientation, rotating the spreading ridges along with 30-40° (Figure 12 d). Afterwards, the ophiolites are obducted on the Arabian continent and squeezed into their present position, which causes the Northern and Central blocks to rotate in a CW sense, and the Eastern blocks in a CCW sense (Figure 12 e).

Evidence for both pre-subduction and post-subduction spreading ridges can be found in the present-day orientations of the sheeted dykes of Oman (Figure 1). The post-subduction sheeted dykes would have overgrown the pre-subduction sheeted dykes, which is why in the central parts of the Oman nappe we find post-subduction sheeted dykes oriented along the nappe, and on the edges of the Oman nappe we find pre-subduction sheeted dykes that are oriented perpendicular to the nappe. Before subduction initiation started, spreading took place in between the transform motions, and later perpendicular to the subduction zone striking E-W (Figure 12 c). Both pre- and post-subduction sheeted dykes were rotated 30-40° CCW along with the subduction zone, which explains why their orientations can still be found perpendicular to each other in the present-day sheeted dykes. This also explains why site FF01 shows an initial dyke orientation that is E-W oriented instead of N-S oriented.

6 Conclusions

The results of this study can be summarised as follows:

The paleolatitude of the studied Oman ophiolite at the moment of formation is 8.6° (±4.8°)N.
The paleospreading ridge is oriented striking rougly N-S (166.9-346.9°, standard deviation 21.3°), with the exception of one location showing an E-W (71.3-251.3°, standard deviation 7.9°) striking orientation. The amount of rotation that the total ophiolite experiences is 30-40° in a CCW sense. The sense of rotation in the northern and central blocks for the sheeted dykes is CW, while the eastern block experiences a CCW rotation.

The Oman ophiolite did not form along a Neo-Tethys ocean spreading ridge, but rather originates from a N-S transform segment along a Neo-Tethys ocean spreading ridge situated above the NE moving Indian plate. A subduction zone formed from a former N-S striking transform fault at the western limit of the Indian plate, above which the N-S striking spreading ridge formed. Overriding spreading and subduction happened in an E-W manner.

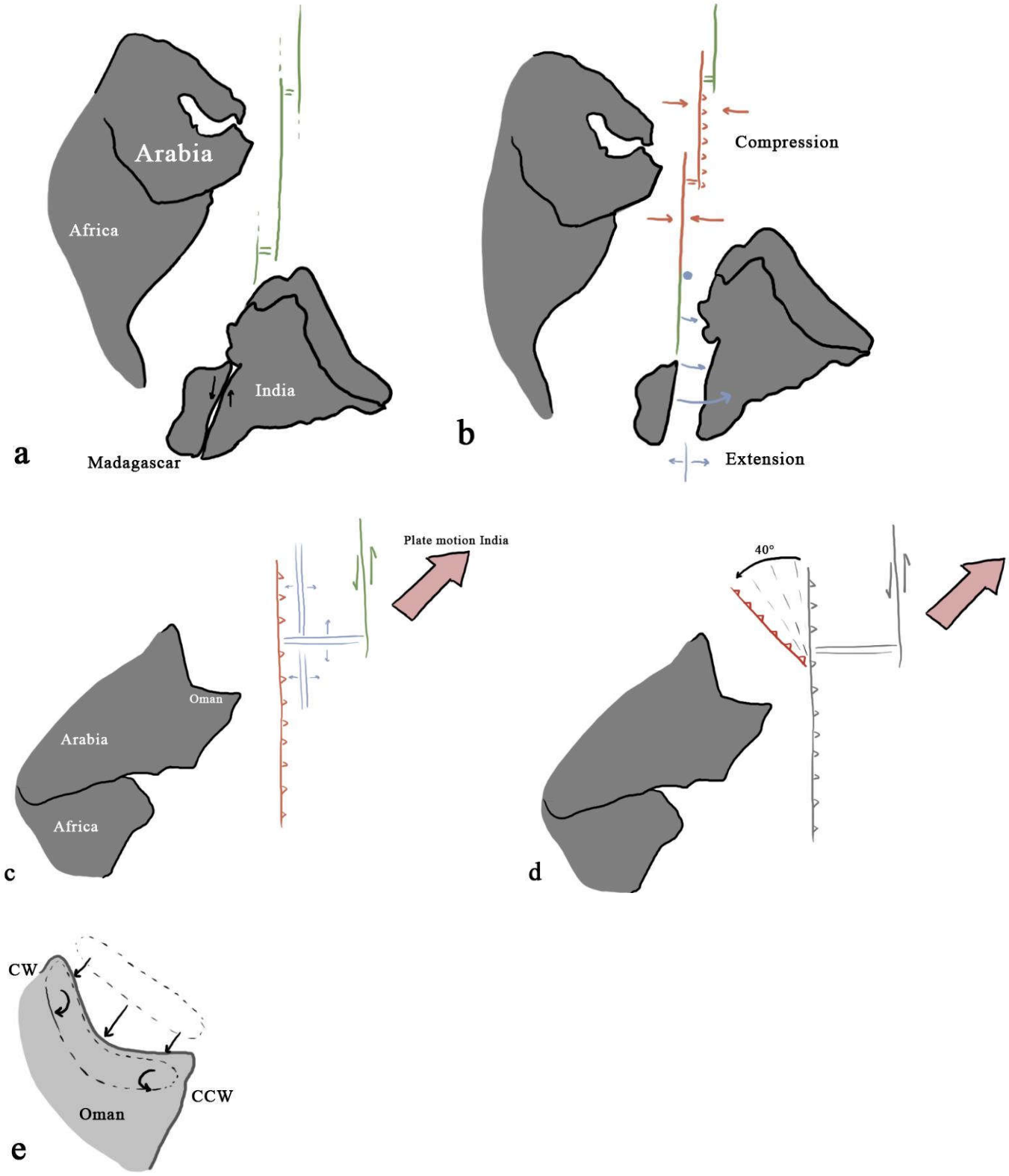

Figure 12. Sketch of our interpretation of the evolution of the Oman ophiolites. Modified after Gaina et al., 2015.

Acknowledgements

First and foremost I would like to thank my two supervisors Dr. Douwe van Hinsbergen and Dr. Marco Maffione of Utrecht University, who always supported me, helped me out whenever I had questions about the research or writing, and who left lots of valuable comments on this thesis. I am very grateful to both, and wouldn't be where I am now without them.

I would also like to thank Dr. Carl Guilmette and Benoit Charette who were involved in the fieldwork for this research. Without their participation, the fieldwork wouldn't have been as great of a success and as much fun. I would like to give special thanks to all the people working at Paleomagnetic Laboratory Fort Hoofddijk (Utrecht) for helping me make sense of my samples in the lab, as well as giving me great times.

I would also like to acknowledge Dr. Al Battashi for providing us with information and permissions during the fieldwork, Mr Saeed for helping us out in Sohar, and Mr. Kaleefi and his family for providing us much-needed fruit and drinks on a particularly hot fieldwork day.

Last but not least, I would like to thank my parents, grandparents, friends, and roommates for always being there for me, providing me unfailing support, and their endless encouragement throughout all of my study years, and for making sure I got –some- relaxation as well. I couldn't have done it without you!

References

Allerton, S., Vine, F.J., 1987. Spreading structure of the Troodos ophiolite, Cyprus: Some paleomagnetic constraints. Geology, v. 15, pp. 593-597.

Boudier, F., Ceuleneer, G., Nicolas, A., 1988. Shear zones, thrusts, and related magmatism in the Oman ophiolite: Initiation of thrusting on an oceanic ridge. Tectonophysics, v. 151, pp. 275-296.

Butler, R.F., 1992. Paleomagnetism: magnetic domains to geologic terranes. Blackwell Scientific Publications, Oxford, 319.

Chadima, M., Hrouda, F., 2006. Remasoft 3.0; a user-friendly paleomagnetic data browser and analyser. Travaux Géophysiques 27, 20-21.

Day, R., Fuller, M., Schmidt, V.A., 1977. Hysteresis properties of titanomagnetites – grain-size and compositional dependence. Phys. Earth Planet. Inter. 13 (4), pp 260-267.

Deenen, M.H.L., Langereis, C.G., van Hinsbergen, D.J.J., Biggin, A.J., 2011. Geomagnetic secular variation and the statistics of paleomagnetic directions. Geophys. J. Int. v. 186; p. 509-520.

Ernewein, M., Pflumio, C., Whitechurch, H., 1988. The death of an accretion zone as evidenced by the magmatic history of the Sumail ophiolite (Oman). Tectonophysics, v. 151, pp. 247-274.

Feinberg, H., Horen, H., Michard, A., Saddiqi, O., 1999. Obduction-related remagnetization at the base of an ophiolite: Paleomagnetism of the Samail upper nappe lower sequence and of its continental substratum, southeast Oman Mountains. Journal of Geophysical Research, v. 104, pp. 17,703-17,714.

Fisher, R.A., 1953. Dispersion on a sphere. Proceedings of the Royal Society of London, Ser. A; v. 217; p. 295-305, doi:10.1098/rspa.1953.0064.

Gaina, C., van Hinsbergen, D.J.J., Spakman, W., 2015. Tectonic interactions between India and Arabia since the Jurassic reconstructed from marine geophysics, ophiolite geology, and seismic tomography. Tectonics, v. 34, pp. 875-906, doi:10.1002/2014TC003780.

Inwood, J., Morris, A., Anderson, M.W., Robertson, A.H.F., 2009. Neotethyan intraoceanic microplate rotation and variations in spreading axis orientation: Palaeomagnetic evidence from the Hatay ophiolite (southern Turkey). Earth and Planetary Science Letters, 280, pp. 105-117.

Kirschvink, J.L., 1980. The least-squares line and plane and the analysis of palaeomagnetic data. Geophys. J. Int., v. 62, pp. 699-718.

Lippard, S.J., Shelton, A.W., Gass, I.G., 1986. The ophiolite of Northern Oman. London, 178 pp.

Lowrie, W., Channel, J.E.T., Alvarez, W., 1980. A review of magnetic stratigraphy investigations in Cretaceous pelagic carbonate rocks. Journal of Geophysical Research, v. 25, pp. 3597-3607.

MacLeod, C.J., Carlut, J., Escartín, J., Horen, H., Morris, A., 2011. Quantitative constraint on footwall rotations at the 15°45'N oceanic core complex, Mid-Atlantic Ridge: Implications for oceanic detachment fault processes. Geochemistry, Geophysics, Geosystems (G3), v. 12, n. 5, pp. 1-29.

Morris, A., Anderson, M.W., Robertson, A.H.F., 1998. Multiple tectonic rotations and transform tectonism in an intraoceanic suture zone, SW Cyprus. Tectonophysics, v. 445, pp. 245-272.

Morris, A., 2009. Footwall rotation in an oceanic core complex quantified using reoriented Integrated Ocean Drilling Program core samples. Earth Planet Sci. Letters, v. 287, pp. 217-228.

Mullender, T.A.T., Velzen, A.J., Dekkers, M.J., 1993. Continuous drift correction and separate identification of ferrimagnetic and paramagnetic contributions in thermomagnetic runs. Geophysical Journal International, 114(3), pp 663-672.

Mullender, T.A.T., Frederichs, T., Hilgenfeldt, C., Fabian, K., Dekkers, M.J., 2005. Fully automated demagnetization and measurement of NRM, ARM and IRM on a '2G' SQUID magnetometer. IAGA, abstract number: IAGA2005-A-00898.

Nicolas, A., Ceuleneer, G., Boudier, F., Misseri, M., 1988. Structural mapping in the Oman ophiolites: Mantle diapirism along an oceanic ridge. Tectonophysics, v. 151, pp. 27-56.

Nicolas, A., 1989. Structures in Ophiolites and Dynamics of Oceanic lithosphere. Kluwer, Dordrecht.

Nicolas, A., Boudier, F., 1995. Mapping oceanic ridge segments in Oman ophiolite. Journal of Geophysical Research, v. 100, pp. 6179-6197.

Nicolas A., Ildefonse, B., Boudier, F., Lenoir, X., Ismail, W.B., 2000. Dike distribution in the Oman-United Arab Emirates ophiolite. Marine Geophysical Researches, v. 21, pp. 269-287.

Pearce, J.A., Lippard, S.J., Roberts, S., 1984. Characteristics and tectonic significance of supra-subduction zone ophiolites.

Geological Society, London, Special Publications 1984, v. 16, p. 77-94.

Pearce, J.A., 2003. Supra-subduction zone ophiolites: The Search for modern analogues. Geological Society of America, Special paper 373, pp. 269-293.

Perrin, M., Prevot, M., Bruere, F., 1994. Rotation of the Oman ophiolite and initial location of the ridge in the hotspot reference frame. Tectonophysics, v. 229, pp. 31-42.

Perrin, M., Plenier, G., Dautria, J-M., Cocuaud, E., Prévot, M., 2000. Rotation of the Semail ophiolite (Oman): Additional Paleomagnetic data from the volcanic sequence. Marine Geophysical Research, v. 21, pp. 181-194.

Pozzi, J.P., Westphal, M., Girardeau, J., Besse, J., Yao, X.Z., Xian, Y.C., Li, S.X., 1984. Paleomagnetism of the Xigaze ophiolite and flysch (Yarlung Zangbo suture zone, southern Tibet); latitude and direction of spreading. Earth and Planetary Science Letters 70, pp. 383-394.

Rioux, M., Bowring, S., Kelemen, P., Gordon, S., Miller, R., Dudás, F., 2013. Tectonic development of the Samail ophiolite: High-precision U-Pb zircon geochronology and Sm-Nd isotopic constraints on crustal growth and emplacement. Journal of Geophysical Research, v. 118, N. 5, pp. 2085-2101.

Robinson, J., Beck, R.A., Gnos, E., Vincent, R.K., 2000. New structural and stratigraphic insights for northwestern Pakistan from field and Landsat Thematic Mapper data. Geol. Soc. Am. Bull., 112, 364-374.

Tauxe, L., 2010. Essentials of paleomagnetism. University of California Press.

Thomas, V., Pozzi, J.P., Nicolas, A., 1988. Paleomagnetic results from Oman ophiolites related to their emplacement. Tectonophysics, v. 151, pp. 297-321.

Tilton, G.R., Hopson, C.A., Wright, J.E., 1981. Uranium-lead isotopic ages of the Samail ophiolite, Oman, with application to Tethyan ocean ridge tectonics. Journal of Geophysical Research, v. 86, pp. 2763-2775.

Vandamme, D., 1994. A new method to determine paleosecular variation. Physics of the Earth and Planetary Interiors 85, 131-142.

Van Hinsbergen, D.J.J., Lippert, P.C., Dupont-Nivet, G., McQuarrie, N., Doubrovine, P.V., Spakman, W., Torsvik, T.H., 2012. Greater India Basin hypothesis and a two-stage Cenozoic collission between India and Asia. PNAS, v. 109, n. 20, pp. 7659-7664.

Zijderveld, J.D.A., 1967. AC demagnetisation of rocks: Analysis of results. Methods in Paleomagnetism. Elsevier, edited by D.W. Collinson et al., p. 254-268.

Table 1. Paleomagnetic results from the Oman Ophiolite.

Site	Lithology	Locality	Str.	Dip[1]	Treatment	Lat	Long	n/N	D	dDx	I	dIx	α95	k	K	A_{95}	A_{95min}	A_{95max}
Sites considered in this study																		
AA01	Sheeted dykes	Wadi Tayin	345	70 E[2]	AF,TH	22 48'36"N	058 34'03"E	22/23	355	6.5	25.0	10.9	8.2	15.4	25.3	6.3	3.5	11.7
AS01	Sheeted dykes	Shaik	145	40 W[3]	AF,TH	24 20'09"N	056 28'36"E	13/18	123	12.3	-46.8	13.1	9.3	20.8	15.5	10.9	4.3	16.3
BB01	Sheeted dykes	Sumail	103	77 S[4]	AF,TH	23 05'02"N	058 10'39"E	35/35	304	4.6	-12.5	8.8	5.5	20.2	29.4	4.5	2.9	8.7
DA01	Sheeted dykes	Miskin	358	38 E[5]	AF,TH	23 37'45"N	056 38'06"E	13/13	010	10.2	-5.2	20.2	17.8	6.4	17.6	10.2	4.3	16.3
FF01	Sheeted dykes	Sarami	165	53 W[4]	AF,TH	23 49'38"N	056 52'46"E	20/32	102	13.2	55.3	10.5	7.9	17.8	10.3	10.7	3.6	12.4
HA01	Sheeted dykes	Fizh	295	47 NE[6]	AF,TH	24 48'29"N	056 17'38"E	17/17	041	6.1	32.9	6.1	6.1	34.9	38.2	5.8	3.9	13.8
HD01	Sheeted dykes	Hilti	006	65 E[7]	AF,TH	24 13'40"N	056 07'53"E	23/27	048	7.4	41.6	9.1	5.9	27.7	21.0	6.8	3.4	11.4
MU01	Sheeted dykes	Fizh	182	34 W[5]	AF,TH	24 30'44"N	056 21'13"E	31/35	358	6.6	52.8	6.6	4.6	31.9	22.9	5.5	3.0	9.4
MA01			331	49 NE[8]														
MA02	Pillow basalts	Shaik	327	58 NE[9]	AF,TH	24 20'34"N	056 30'27"E	33/34	084	4.8	16.8	8.8	5.9	19.0	29.2	4.7	3.0	9.1

[1] Fischer mean
[2] Averaged over 10 dykes, with a slightly shallowing dip to the east
[3] Averaged over 9 dykes
[4] Averaged over 6 dykes
[5] Averaged over 8 dykes
[6] Averaged over 11 dykes, some sills crosscutting them
[7] Averaged over 11 dykes
[8] Averaged over 6 directions
[9] Averaged over 5 directions

Abbreviations: n is the number of specimens used in the statistics; N is the total number of specimens processed; D = declination; **I** = inclination; dDx = error margin of declination; d**I**x = error margin of inclination; α95 = radius of the 95% confidence cone of the site-mean direction for characteristic remanent magnetisation (ChRM); k = Fisher parameter for characteristic remanent magnetisation (ChRM); A95 = radius of the 95% confidence cone of the site-mean direction for virtual geomagnetic pole (VGP); K = Fisher parameter for virtual geomagnetic pole (VGP); TH = thermal demagnetisation; AF = alternating field demagnetisation.

Table 2. Net Tectonic Rotation (NTR) results from the Oman Ophiolite.

	NTR Analysis	AA01	AS01	BB01	DA01	FF01	HA01	HD01	MU01
		Sheeted dykes	Sheeted dykes	Sheeted dykes	Sheeted dykes	Sheeted dykes	Sheeted dykes	Sheeted dykes	Sheeted dykes
Preferred Solution 1	Reference Direction[1]	00001/16.8	00001/16.8	00001/16.8	00001/16.8	00001/16.8	00001/16.8	00001/16.8	00001/16.8
	In situ dec/inc[2]	355/25	123/-47	303.5/-12.5	010/-5	102/55	40.6/32.9	048/42	358/52.8
	Dyke Margin, str/dip ° [3]	344.9/70	145/40	102.8/77.3	358/38	165/53	294.5/46.9	006/65.4	181.6/33.7
	Azimuth Rotation Axis	18.8	187.1	203.7	162.7	314.6	9.3	236.3	325.6
	Plunge Rotation Axis	30	50.8	54.8	3.6	65.1	42.2	26.6	28
	Rotation	25.8 CCW	144.8 CW	66.8 CCW	52.9 CW	103 CW	97.8 CW	50.8 CW	66.3 CW
	Initial Strike dyke/bedding	179.7	156.6	163.4	169.2	71.3	14.2	170.9	138.9
	Initial Dip dyke/bedding	90	90	90	90	90	90	90	90
	Iteration average strike	174.5	156.4	163.4	167.8	70.2	14.0	170.6	138.9
	Standard deviation avg. strike	5.9	7.2	5.7	10.9	7.9	6.8	5.7	6.4
Solution 2	Reference Direction	00001/16.8	00001/16.8	00001/16.8	00001/16.8	00001/16.8	00001/16.8	00001/16.8	00001/16.8
	In situ dec/inc	355/25	123/-47	303.5/-12.5	010/-5	102/55	40.6/32.9	048/42	358/52.8
	Dyke Margin, str/dip °	344.9/70	145/40	102.8/77.3	358/38	165/53	294.5/46.9	006/65.4	181.6/33.7
	Azimuth Rotation Axis	356.6	78.6	330.7	11.2	247.9	28.4	17.9	5.1
	Plunge Rotation Axis	20.4	15.4	4.8	8.1	10.6	6.5	35.7	35
	Rotation	155.9 CW	133.3 CW	171.6 Either	126.6 CW	88 CW	88.2 CCW	157 CW	154 CCW
	Initial Strike dyke/bedding	0.3	25.4	18.6	12.8	110.7	167.8	11.1	43.1
	Initial Dip dyke/bedding	90	90	90	90	90	90	90	90

[1] The reference direction is the paleohorizontal, obtained from pillow basalts from site MA01-02.
[2] The in situ vector is the geographical declination/inclination from the site, obtained by a 45-cutt-off.
[3] The dyke margin is the Fisher mean dyke orientation in the field, calculated from several dykes (chilled margins). See *Table 1*.